A LATE PLEISTOCENE TO EARLY HOLOCENE CLIMATE, VEGETATION AND FIRE HISTORY RECORD FOR THE BONNEVILLE BASIN, UTAH, USA

by

Kelsey Ann Howard

A thesis submitted to the faculty of
The University of Utah
in partial fulfillment of the requirements of the degree of

Master of Science

Department of Geography

The University of Utah

May 2016

The University of Utah Graduate School

STATEMENT OF THESIS APPROVAL

The thesis of **Kelsey Ann Howard**

has been approved by the following supervisory committee members:

Andrea R. Brunelle	, Chair	**12/9/15** Date Approved
Kathleen Nicoll	, Member	**12/9/15** Date Approved
Isaac Hart	, Member	**12/9/15** Date Approved

and by **Andrea R. Brunelle** , Chair/Dean of

the Department/College/School of **Geography**

and by David B. Kieda, Dean of The Graduate School.

ABSTRACT

The Bonneville basin of northwestern Utah acts as a significant source of paleoenvironmental data due to the sedimentary and geomorphic evidence left behind from the late Pleistocene Lake Bonneville. Macroscopic charcoal and pollen from wetland sediments of North Redden Springs, Utah (40˚ 00’ 47.1” N 113˚ 41’ 59.9” W) were used to reconstruct a record for past environmental and climatic changes during the last 36.8 cal ka BP. Changes in charcoal deposition rates (particles/cm^2/yr), peak magnitudes (calculated using Char Analysis), and percentages of total pollen were used to interpret the fire, vegetation, and climate dynamics. Additionally, distinct shifts in the magnetic susceptibility and loss-on-ignition of sediments were used to understand past lacustrine events in the basin. During the late Pleistocene (36.8–29 cal ka BP), a cold/dry adapted sagebrush steppe surrounded Lake Bonneville, with no fire episodes near the study site due to the inundation of the site by Lake Bonneville. A subsequent increase in winter precipitation from the southward shift of the jet stream during the latest Pleistocene (29–16 cal ka BP) resulted in the expansion of a conifer forest and deeper lake levels. One fire episode occurred at 21 cal ka BP and is associated with a wet period followed by warming. Greater fuel loads correspond to increased fire episodes during the middle and early Holocene (16–6.0 cal ka BP). As early as 16 cal ka BP, a xeric shrub steppe composed of halophytic Amaranthaceae and Sarcobataceae vegetation dominated large expanses of playa surrounding the North Redden spring-wetland complex. The late

Holocene (6.0 cal ka BP–present) was characterized as a period of increased aridity, interspersed with cool-wet episodes. A xeric shrub steppe expanded its range to become the dominate vegetation type on the landscape. Increases in aquatic plants and other diversified vegetation types occurred in response to heightened amounts of summer moisture. Fires continued to increase in frequency and intensity throughout the historical period. Mechanisms behind fire activity likely included wet climate episodes followed by dry climate episodes. Additionally, anthropogenic burning, fire suppression, and invasive plant species may have contributed to increased fire activity.

TABLE OF CONTENTS

LIST OF FIGURES

Figure Page

ACKNOWLEDGEMENTS

I would like to thank my advisor Andrea Brunelle, for providing me with the support, encouragement, and confidence to continue my education as a graduate student and for providing me with the opportunity to excel in my research and class work. I thank my committee, Isaac Hart and Kathleen Nicoll, for offering important input and guidance. A special thank you to my fiancé Scott for endless emotional support throughout my time at the University of Utah and to my cats for their reassuring meows. Also, many thanks to Dugway Proving Ground Archaeologists, Jennifer DeGraffenried and Nate Nelson for providing me with helpful archaeological information and access to the Dugway Proving Ground for the collection of amazing sediment cores. Thanks to Bruce Kiaser for elemental analysis assistance and insightful discussions. I would also like to thank Jennifer Watt for introducing me to the field of Paleoecology, and thanks to the RED lab for laboratory assistance. Thank you Dugway Proving Ground (National Defense Grant) and Argonne National Laboratories for funding. Lastly, thank you to those who assisted with the fieldwork, and the many others who offered their support and kindness.

INTRODUCTION

The Bonneville Basin extends across northwestern Utah, northeastern Nevada and southeastern Idaho, making it the largest drainage basin within the Great Basin of western North America (Fig. 1). The basin has been extensively studied since the late 1800s (e.g., Currey et al., 1983; Eardley et al., 1973; Gilbert, 1890; Malde, 1968; Oviatt et al., 1992; Scott et al., 1983;) and is a prominent source of paleoenvironmental data due to the alluvial and geomorphic evidence left behind from the late Pleistocene Lake Bonneville (Patrickson et al., 2010). Lake Bonneville was one of the largest pluvial paleolakes to exist and fluctuate in the Great Basin from 30 to 12 thousand calibrated radiocarbon years before present (cal ka BP). The major phases of Lake Bonneville have been well documented and demonstrate detailed knowledge of lake levels (Oviatt, 1997; Oviatt 2015; Oviatt et al., 1992), although important time periods of the formation of Lake Bonneville and of late regressive phase (see definition, p.10 below) require additional refinement (Godsey et al., 2005).

The detailed information of Lake Bonneville's shorelines, oscillations, and the timing of the Bonneville flood have led to paleoclimate investigations (Benson et al., 2011; Godsey et al., 2005, 2011; Laabs et al., 2009; Munroe et al., 2006; Oviatt, 1997; and Spencer et al., 1984), as well as studies of terrestrial environmental change through regional pollen sequences (Beiswenger, 1991; Bright, 1966; Davis, 2002; Jimenez-Moreno et al., 2007; Madsen and Currey, 1979; Mehringer, 1985; Spencer et al., 1984;

and Thompson, 1992). In addition to these paleoenvironmental studies, packrat middens (Rhode, 2000 a, b; Rhode and Madsen, 1995a, b; Thompson, 1990), faunal records (Broughton, 2000; Broughton et al.,2000; Grayson, 1998, 2000a, b; Schmitt et al., 2002), geomorphic records (Oviatt et al., 2003; Oviatt et al., 2005), and fire history studies (Mensing, 2006; Patrickson et al., 2010), as well as archaeological records of human occupation (Louderback et al., 2010; Massimino and Metcalfe, 1999) have contributed to a detailed record of fluctuations in hydrologic balance, terrestrial biotic distributions and patterns of land and resource use by human inhabitants in the Bonneville basin (Louderback and Rhode, 2009).

The previous palynological studies of the Bonneville basin's lake and marsh sediments have demonstrated consistent trends in vegetation as indicators of regional climate and hydrology (Beiswenger, 1991; Bright, 1966; Louderback and Rhode, 2009; Madsen and Currey, 1979; Mehringer, 1985; Spencer et al., 1984; Thompson, 1992). However, these earlier records contain coarse temporal resolution, and consequently overlook important periods of environmental change, including the late Pleistocene, the Bonneville Flood, and the Pleistocene/Holocene environmental transition. Additionally, there still exists a lack of understanding concerning the chronology of Lake Bonneville and the extent of climate, fire, and vegetation change impacting prehistoric human occupation in the basin, despite the extensive knowledge regarding the geomorphic, paleoclimatic, and, the robust archaeological record for the area.

An understanding of the local and regional climate system, as well as the vegetation, fire, and sedimentation dynamics of the Bonneville basin is important for determining both the chronology of Lake Bonneville and the impact these changes had on

prehistoric people. This study will contribute to the emerging body of work on the gradual and abrupt environmental changes occurring in the Bonneville basin during the last 36. 8 cal ka BP through a sedimentary analysis of the NRS14A core from North Redden Springs, a ~1000-acre spring marsh complex located on the southwestern margin of the Great Salt Lake desert (Fig. 2). The core provides a nearly continuous record of wetland and lacustrine deposits from Lake Bonneville and presents an opportunity to examine environmental changes through the late Pleistocene and Holocene in the Bonneville basin (Fig. 3). Additionally, dozens of early- and late-period archaeological sites are found near the spring complex on Dugway Proving Ground lands. Thus, the North Redden Springs record from core NRS14A will further aid in understanding the development of wetland systems that were essential for these Paleoindian and late Holocene occupations. The long-term records of fire, vegetation and climate will assist Dugway Proving Ground (DPG) archaeologists in evaluating how variations in spring activity, and environmental conditions impacted these prehistoric human populations. Furthermore, the sediment record will provide a baseline of fire frequency and vegetation change for land managers operating in the Bonneville basin.

Objectives

In order to fully understand how the Bonneville basin has responded to past climatic, hydrologic and biotic changes throughout the last ~37,000 years, this study has reconstructed the local history of fire, vegetation, and climate for North Redden Springs, as well as contributed to the chronology of Lake Bonneville. These reconstructions are based on the principle that the closed-basin system of Lake Bonneville-Great Salt Lake is a climate-forced hydrologic system with an enormous capacity to store information on

past history (Currey and Oviatt, 1985). A multiple proxy analysis that examines the record of climate change preserved in sediments of Lake Bonneville is important for refinement of the lacustrine record, and for the reconstruction of fire and vegetation histories for the region. Additionally, the timing and frequency of pluvial events in the Great Basin provides further data regarding how changes to the climate have impacted sensitive lake and wetland systems in the past. The following are the specific research objectives for this study:

1. Describe the paleoenvironmental history of the last 36,800 years for the North Redden Springs Region of the Bonneville Basin.
2. Assess the paleoenvironmental data to potentially refine the chronology of Lake Bonneville lake levels.
3. Describe how the paleoenvironmental context may have impacted prehistoric human populations within the region.

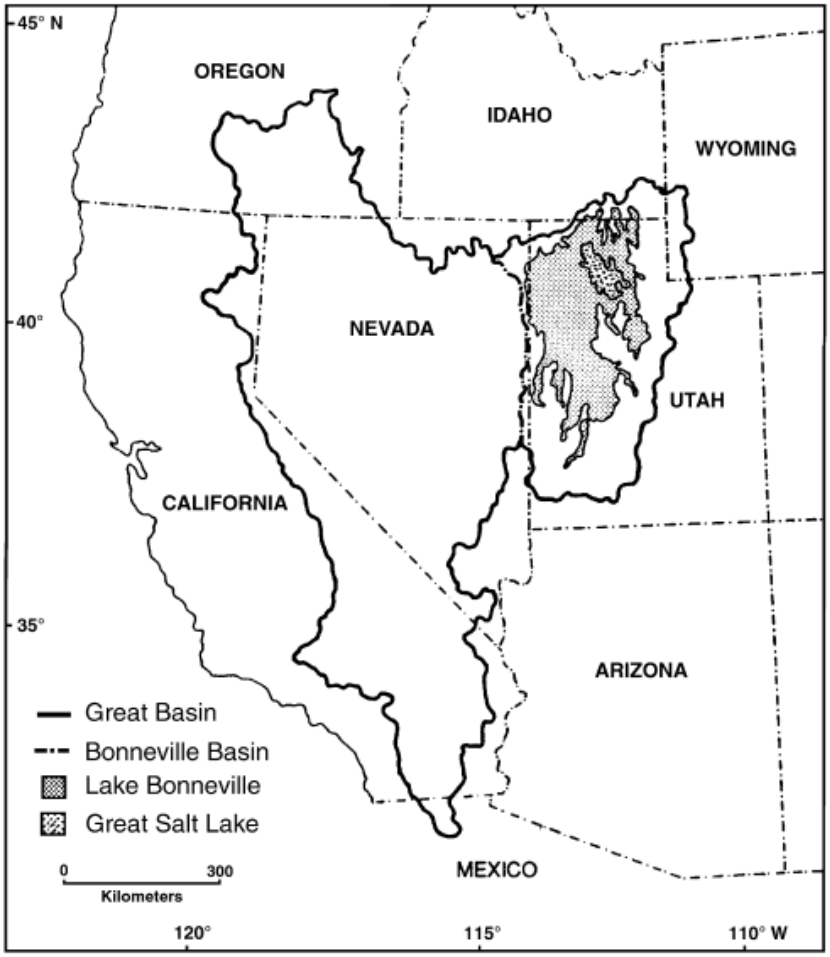

Figure 1. Location of the Great Basin, Bonneville Basin, and Great Salt Lake, USA (from Madsen et al., 2001).

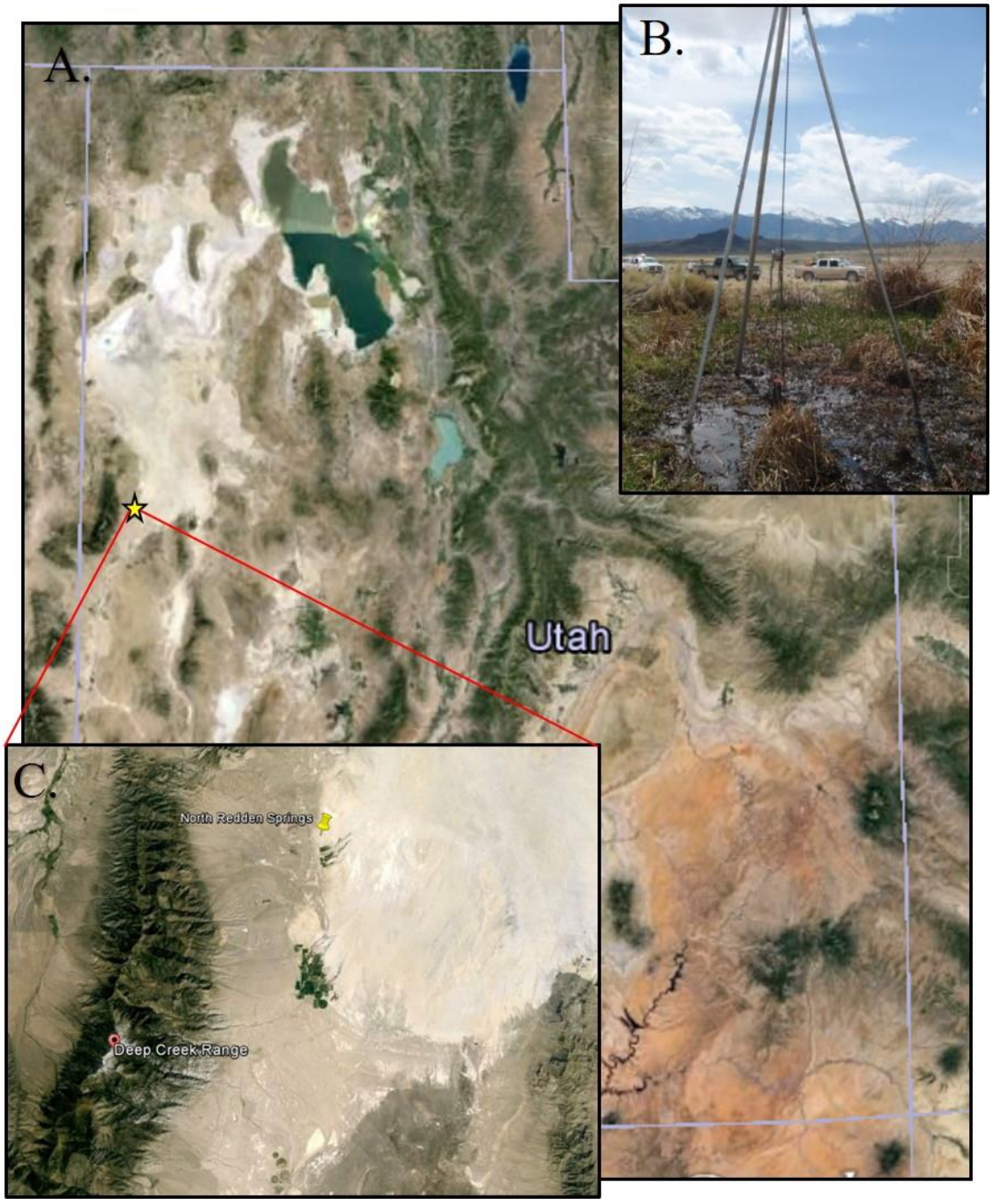

Figure 2. Satellite images of study site, (A) Satellite image of Utah. Star marks location of study site, (B) The North Redden coring site facing west towards the Deep Creek Mountains, Bonneville basin, Utah, (C) Satellite image of the North Redden Spring study site (Google Inc., 2015).

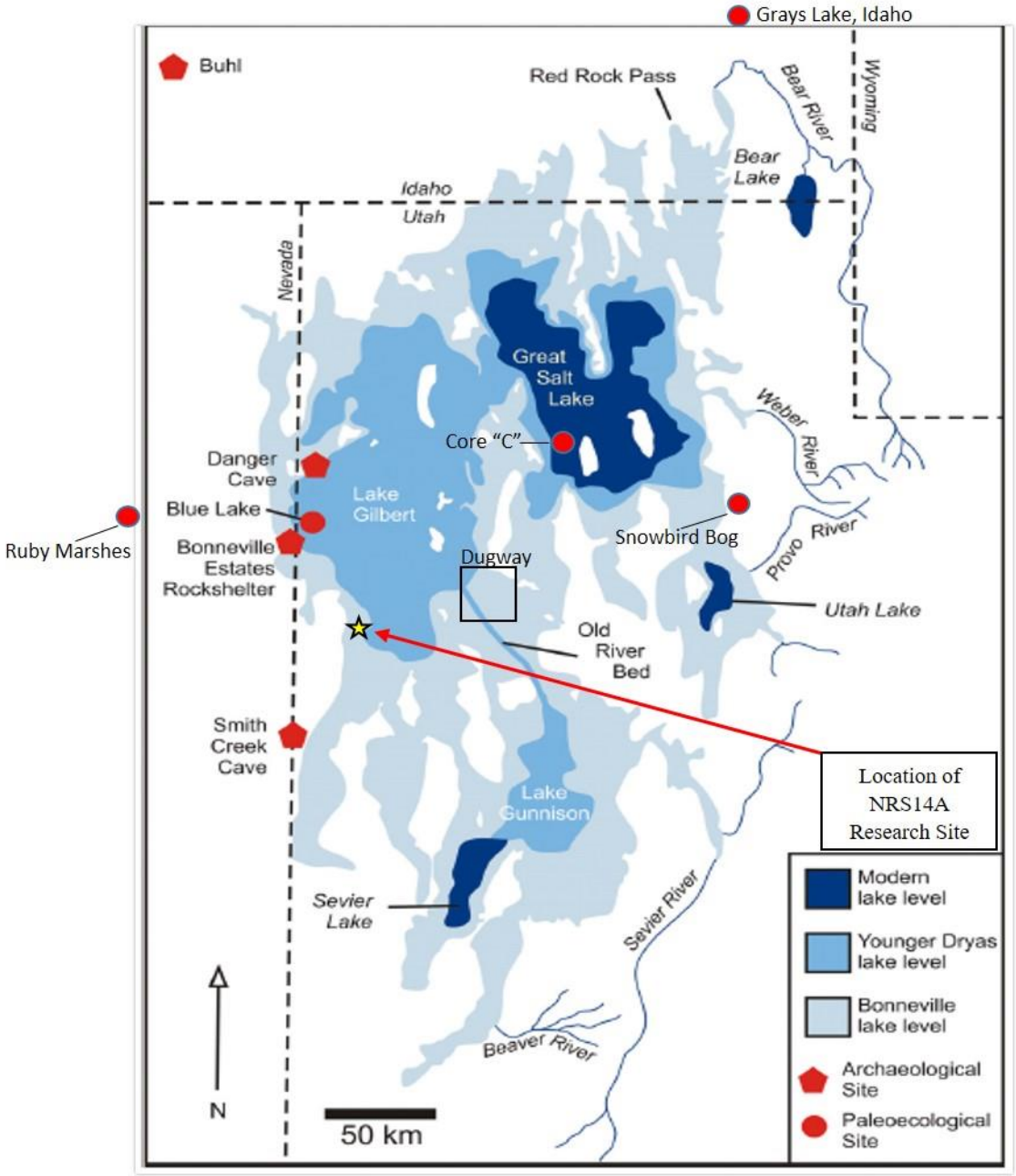

Figure 3. Extent of late Pleistocene pluvial lakes of the Bonneville Basin at 18.7 cal ka BP (Bonneville lake level), 12.5 cal ka BP (Younger Dryas lake level) and modern lake level (Goebel et al., 2011). Modified from Oviatt et al. (2002).

SITE DESCRPITION

Geology/Geography of Bonneville Basin

With an area of 135,000 km², the Bonneville drainage basin is the largest and deepest sub-basin located in the easternmost catchment of the North American Great Basin (Fig. 1; Nishizawa et al., 2013). The paleogeographically defined Bonneville lake basin, or the pluvial lake basin that once contained Lake Bonneville, constitutes a major part of the Bonneville drainage basin. For this reason, the term "Bonneville basin" is used to specify the Bonneville lake basin, and not the Bonneville drainage basin (Nishizawa et al., 2013). The Bonneville basin was first described by Gilbert (1890), who observed that the province was characterized by a series of north-south trending fault-block mountains separated by arid, flat valleys of Tertiary strata and Quaternary alluvium. Strike-slip and extensional faulting of the North American and the Pacific Plates began forming this internally drained basin ~15 million years ago, and the basin continues to develop today (Madsen, 2000).

The Bonneville basin is bordered by the Raft River Mountains to the north and the Pilot Range and Deep Creek Range to the west. The larger Wasatch Range forms the basin's eastern margin. The major fault-block mountains within the Bonneville basin include the Oquirrh, Stansbury, Promontory, Grouse Creek and Cedar Mountains, with smaller mountain ranges of lower elevations dispersed throughout the basin. On the western edge, Cambrian bedrock outcrops, as well as Devonian carbonate rocks are

present, along with older quartzite and younger limestone formations. Igneous intrusive rocks also occur in the area, such as the major granite intrusive complex located in the Deep Creek Range. Additionally, the western margin of the basin is spotted with tertiary volcanics, including a major source of obsidian located on Topaz Mountain along the southern edge of the Great Salt Lake Desert (Madsen, 2000).

Lake Bonneville

The geomorphology below elevations of 1700 m in the Bonneville basin is largely the result of the late Pleistocene rise and fall of Lake Bonneville (Madsen, 2000). Lake Bonneville was a large freshwater lake in the extensional-tectonic basin that has been occupied in modern times by the Great Salt Lake in the eastern Great Basin (Fig. 3; Oviatt, 2015). The lake had a maximum depth of 372 m and an area of 50,000 km², spanning 450 km from north to south and 200 km from east to west (Goebel et al., 2011; Patrickson et al., 2010). The Pleistocene lake was fed by the snowmelt through perennial rivers originating in the Wasatch and Uinta Mountain Ranges, including the Bear, Weber, and Provo Rivers in the Great Salt Lake basin and the Sevier and Beaver Rivers in the Sevier basin (Oviatt, 2015).

The initial rise of Lake Bonneville is considered to have occurred around 30.5 cal ka BP, when the lake quickly rose over 80 m in a very short time period due to the diversion of the upper Bear River as a result of the Hansel Valley volcanic eruption (Reheis et al., 2014). Previous studies have examined the mechanisms behind the expansion of Lake Bonneville (Antevs, 1948; Hostetler et al., 1994; Kaufman, 2003; McGee et al., 2012; Oviatt, 1997). The growing consensus is that pluvial lake level changes during the Wisconsin ice age in the Great Basin, including the Bonneville basin,

were affected by the changing size of the Cordilleran and Laurentide ice sheets, as well as a permanent high-pressure area that resulted in a southward shift of the jet stream's mean path to increase regional winter precipitation (Nishizawa et al., 2013). The shift in the jet stream over the Great Basin had a powerful impact on the region's water balances as precipitation was further enhanced by "lake effect storms." The orographic enhancement of precipitation by the Wasatch Mountains subsequently resulted in increased lake size and glacial extent (Benson et al., 2011; Oviatt, 2007). Lyle et al. (2012) have proposed a different atmospheric-oceanic circulation mechanism to suggest that the large Great Basin lakes during the Last Glacial Maximum (LGM) and the last deglaciation might have instead resulted from the increase in moisture transported from the tropical eastern Pacific and the Gulf of Mexico during the spring/summer ("the summer monsoon hypothesis"). However, Nishizawa et al. (2013) concluded that a combination of factors impacted the hydrological/climate systems of Lake Bonneville. The region was dominated by enhanced spring/summer precipitation from tropical eastern Pacific air masses between ~50 – 28 cal BP ("the summer monsoon hypothesis"), and a subsequent shift of the westerly winter storm tracks at ~28–14 cal BP (LGM), which increased precipitation to thus form Lake Bonneville in western Utah/eastern Nevada.

The history of Lake Bonneville since the LGM can be divided into three major periods: the transgressive phase, the overflowing phase, and the regressive phase (Fig. 4; Currey, 1990; Oviatt, 2015). The lake occupied a hydrographically closed-basin during the transgressive phase at ~25 cal ka BP, in which all the water coming into the system from direct precipitation, river runoff, and groundwater exited the basin through evaporation (Oviatt, 2015). This hydrologically closed-basin was sensitive to changes in

climate, and thus the lake underwent a series of lake level oscillations, commonly known as the Stansbury Oscillation, as a result of changes in its water budget. According to Oviatt (2015), the lake reached its high point at 18.4 cal ka BP to form the Bonneville Shoreline. Subsequently, the lake began the overflow phase when the lowest point on the natural dam was washed out on the basin rim near Red Rock Pass, ID. The catastrophic collapse of the alluvial fan dam resulted in the Bonneville flood at 18.6–17.1 cal ka BP (rounded to 18 cal ka BP), which caused the lake to drop by over 130 m in less than a year as water rushed out of the basin into the Snake Drainage. The lake subsequently flowed out of the basin in the form of a river and swept across a wide and rising threshold on landslide deposits for three thousand years (Oviatt, 2015). Following this overflowing phase, the Provo shoreline developed in the basin as the lake transitioned to the regressive phase and returned to a closed-basin. The timing of the end of the Provo-shoreline formation has been suggested by Godsey et al. (2011) to be 15 cal ka BP, while Miller et al. (2013) argue that it occurred earlier, at ~16.7 cal ka BP. This discrepancy is still not resolved. However, Oviatt (2015) suggests that the shoreline is older than 14 cal ka BP. During this regressive phase, the lake dropped rapidly to an elevation of 1280 m, comparable to those of the modern Great Salt Lake by about 13 cal ka BP. The lake eventually split into two sub-basin fresh water lakes: an overflowing lake in the Sevier basin (Lake Gunnison) and a rapidly regressing lake in the Great Salt Lake basin (Lake Gilbert).

During the Younger Dryas, Lake Gilbert transgressed to an elevation of approximately 1300 meters above sea level (masl) and subsequently stabilized at the Gilbert shoreline. At this time, Lake Gunnison overflowed to the North at the Old River

Bed Threshold (Fig. 3), forming extensive marshlands at the Old River Bed Delta. Once the Younger Dryas ended at approximately 11.0–10.2 cal ka BP, Lake Gunnison retreated, the Old River Bed desiccated and Lake Gilbert fell below 1287 masl to form the Great Salt Lake (Goebel et al., 2011). In addition, shallow lakes, marshes, and wet meadows began forming on valley floors once the lake evaporated, and a large volume of ground water previously stored in piedmont and mountain aquifers was discharged onto the basin floor (Reheis et al., 2014). These wetland ecosystems supported significant numbers of Paleoindians as early as 12–11 cal ka BP (Oviatt et al., 2003). Following the retreat of these marsh systems after 9ka, human populations declined in the basin and remained relatively low throughout the mid-Holocene until the expansion of late prehistoric hunter/gatherers after 2.0 cal ka BP (Louderback and Rhode, 2009; Louderback et al., 2010).

Modern Climate and Vegetation

There are several factors influencing the climate of the Bonneville basin, including the position of the jet stream creating a west-to-east air flow, as well as orographic effects from variation in altitude (Madsen, 2000). Currey (1991) defines the climate regime of the Bonneville basin as a geographically and temporally half arid, half humid climate, or a hemiarid environment. As an example, the modern Great Salt Lake Desert receives ~13 cm in annual precipitation while the nearby Wasatch Range averages ~155 cm of annual precipitation. Another climatically important factor is the influence of "lake effect" enhancement of winter precipitation. "Lake effect" storms are generated from the northwesterly orientation of the jet stream that acts to direct cold air masses along the warm, humid lake, and thus causes the cold air masses to become saturated

with water vapor. Once these winter storms reach the Wasatch Mountains, orographic uplift occurs to cause precipitation in the form of snow. This subsequently enhances the amount of precipitation along the eastern basin and produces a regional climate regime of cool, dry valley floors with limited precipitation and cold, wet mountains with higher precipitation (Madsen, 2000).

Precipitation sources for the basin floor originate from the central-northern Pacific storm systems, with small amounts contributed from the Gulf of California and the Gulf of Mexico. There is considerably more precipitation during the winter months to create an uneven year-around precipitation pattern. Typically, higher amounts fall in the spring months of March-May and lesser amounts occur in the summer months of July-September (Madsen, 2000). Seasonal temperatures vary due to the morphology of the Basin and Range, Table 1.

North Redden Springs (N 40˚00’47.1” W 113˚ 41’ 59.9”) is located at the eastern base of the Deep Creek Range on the valley floor of the Great Salt Lake Desert, at approximately 1,284 m elevation (Fig. 2). The spring’s semiarid (or hemiarid) climate contributes to a Northern Desert Shrub Biome with a vegetation regime composed of halophytic playa-margin plants, such as pickleweed (*Allenrolfea occidentalis*), samphire (*Salicornia* spp.) and seepweed (*Suaeda* spp.) that eventually give way to communities dominated by greasewood (*Sarcobatus vermiculatus*) and saltbrush/shadscale (*Atriplex* spp.) (Madsen, 2000). At the location of the coring site, non-native species were present, such as Russian olive (*Elaeagnus angustifolia*), as well as native, saline-tolerant species that included rabbitbrush (*Ericameria nauseosa*), greasewood, pickleweed, along with aquatics including common reed (*Phragmites australis*), and sedges *(Eleocharis spp.*).

The vegetation surrounding the spring becomes sparse as the playa expands across the valley to slowly transition to foothill communities of sagebrush (*Artemisia*), horsebrush (*Tetradymia* spp.) and rabbitbrush, with a range of grasses from bluegrass (*Poa* spp.), wheatgrass (*Agropyron* spp.) and wild rye (*Elymus* spp.). Above the valley and lower foothills, pinyon/juniper woodlands persist in the western ranges at elevations of ~1600 to 2300 masl. Sagebrush/grassland communities are common throughout this woodland zone. At higher elevations (greater than ~2300m), subalpine forest communities of xeric conifers, such as Douglas fir (*Pseudotsuga menziesii)*, white fir (*Abies concolor*), and limber pine (*Pinus contorta*) are present, while mesic species of subalpine fir (*Abies lasiocarpa*) and Engelmann spruce (*Picea engelmannii*) appear on north-facing slopes and drainages. Quaking aspen (*Populus tremuloides*) is also common the subalpine zone, as well as snowberry (*Symphoricarpos* spp.), currant (*Ribes* spp.), buffaloberry (*Shepherdia* spp.), and several species of juniper (*Juniperus* spp*;* Madsen, 2000).

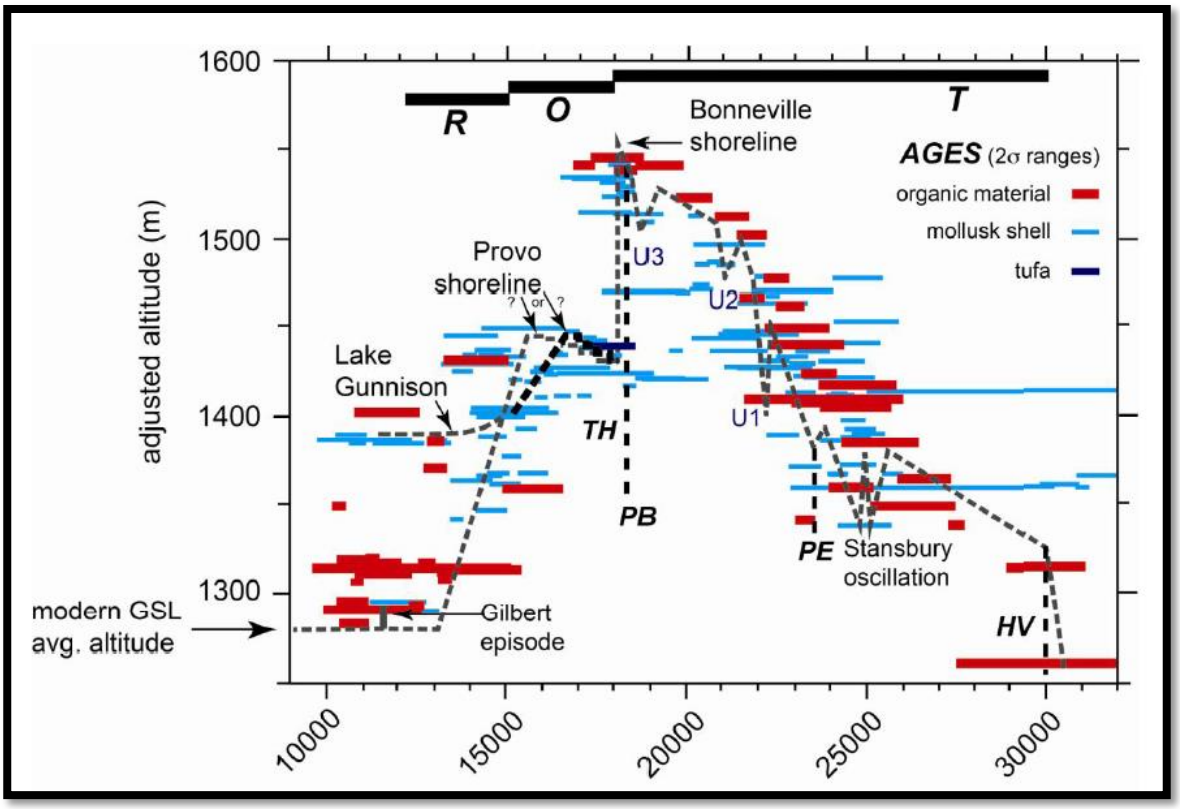

Figure 4. Plot of calibrated ages using altitudes adjusted for isostatic rebound. The transgressive phase (T), overflowing, Provo-shoreline phase (O), and regressive phase (R) are marked with the bold black lines at the top of the figure. Basaltic ashes: HV= Hansel Valley; PE= Pony Express; PB= Pahvant Butte; TH= Tabernacle Hill (Oviatt, 2015).

Table 1
Great Salt Lake Basin Precipitation and Temperature

Table II

Monthly average precipitation (cm) and temperatures (°C) at four stations along a west-to-east transect through the Great Salt Lake basin

Precipitation												
Locality	**Jan**	**Feb**	**March**	**April**	**May**	**June**	**July**	**Aug**	**Sept**	**Oct**	**Nov**	**Dec**
Wendover	0.61	0.33	0.48	1.42	2.48	1.80	0.79	2.11	2.00	2.06	1.73	1.47
Tooele	2.72	3.40	5.90	6.32	4.85	2.82	2.33	2.39	3.60	4.60	4.30	3.76
Salt Lake	2.82	3.12	4.85	5.38	4.57	2.36	2.06	2.18	3.25	3.66	3.28	3.57
Brighton	12.50	12.10	13.54	11.35	7.54	4.47	4.30	4.88	6.55	8.74	12.45	12.50
Temperature												
Locality	**Jan**	**Feb**	**March**	**April**	**May**	**June**	**July**	**Aug**	**Sept**	**Oct**	**Nov**	**Dec**
Wendover	-2.9	0.9	5.6	10.3	16.0	21.6	26.5	24.8	18.6	11.1	3.6	-2.4
Tooele	-1.8	1.0	4.8	9.3	14.5	19.8	24.4	23.1	17.6	11.0	4.1	-1.2
Salt Lake	-2.3	1.2	5.4	9.8	14.8	20.6	25.5	24.2	18.4	11.7	4.8	-1.3
Brighton	-7.2	-6.1	-4.1	-0.2	4.7	10.0	14.5	13.6	8.8	3.5	-2.8	-6.8

Monthly average precipitation (cm) and temperatures (˚C) at four stations along a west-to-east transect through the Great Salt Lake Basin (Madsen, 2000).

METHODS

A multiproxy analysis of wetland sediments collected from North Redden Springs was used to reconstruct the fire and vegetation histories of the Bonneville Basin. These proxies provide information on past spring productivity, lake level fluctuations, as well as the response of vegetation to fire and climate changes. The following analysis techniques were applied a) calculation of charcoal influx as a proxy for fire frequency, b) calculation of pollen percentage and pollen ratios as a proxy for climate change, and c) pollen analysis as a proxy for the local and regional vegetation change over time. Additionally, data obtained from loss-on-ignition analysis and magnetic susceptibility will allow for a better understanding of the hydrological and erosional fluctuations in the region during the last ~36.8 cal ka BP.

Field Methods

Fieldwork, which involved coring two springs, was completed in May 2014 on the southwestern margin of the Great Salt Lake Desert. The North Redden Spring coring location was chosen based on the relatively undisturbed and depositional environment of the spring, as well as its close proximity to archaeological sites (Fig. 2). The field crew consisted of 10 researchers from the University of Utah Records of Environment and Disturbance (RED), and archaeologists from Dugway Proving Ground, as well as

colleagues from Argonne National Laboratories, under the direction of Dr. Andrea Brunelle.

Sediment Coring

Field extraction of the sediment core from North Redden Springs (NRS14A) was conducted using vibracoring techniques to successfully extract the saturated desert sediments. The coring process was completed by attaching a 5-meter-long aluminum core tube to a vibracore head that was powered by a gas motor. The force of gravity and the effects of vibration energy from the vibracore head allowed the aluminum tube to be driven down into the sediment. To the surprise of the field crew, the aluminum core tube entered the sediment with little to no difficulty, suggesting sediment consisting of saturated/organic and/or clay material in contrast to the typical sand and gravel sediments of desert wetlands. Extracting the tube proved difficult due to the vacuum created by the dense, nonporous clay. The NRS14A core recovered 3.82 meters of sediment, with the remaining portion of the tube manually filled with water and capped to generate suction to avoid mixing of the sediment during extraction from the spring. The core was removed from the ground with the assistance of a chain hoist and transported to the (RED) lab to be stored in a cooler at ~1° C.

Laboratory Methods

Once the core was transported to the University of Utah RED lab, the aluminum tube was cut in half length-wise using a circular saw. The 3.82-meter-long core was then sliced in half length-wise in order to preserve half of the core as an archival core for later

interpretation of the laminae from Lake Bonneville. The other half of the core's lithology was described and recorded for color using the Munsell soil color chart and subsampled at contiguous 1-centimeter increments. The 1-centimeter samples were then placed in whirl- packs and stored in a cooler at the RED lab at ~1°.

Chronology

The chronology of the sediment core was completed through processing 23 pollen samples (4cc's each) for AMS ^{14}C dates to establish chronological control and to provide an age model for sediment, charcoal, and pollen accumulation rates. Samples were processed by standard palynological methods reported in Faegri et al. (1989), with the exception that acetolysis is replaced by a 2-minute treatment using Schulze's reagent (HNO_3 and $KClO_3$) to avoid possible Carbon contamination by acetic acid. This method concentrates pollen, proving a good source of organic material for radiocarbon dating in the absence of other terrestrial or aquatic macrofossils. The selection of the initial samples was based on visible changes in the stratigraphy of the core. Subsequent samples were selected corresponding to the timing of Lake Bonneville's transgressive, overflowing, and regressive phases (Oviatt, 2015), as well as the presence of significant archaeological sites in the area (J. DeGraffenried, personal communication, May 8, 2014). The samples were sent to the Center for Applied Isotope Studies (CAIS) in Georgia to be dated according to the AMS methods of the laboratory. Radiocarbon dates were calibrated using the CALIB 7.0 and 7.1 calibration program and were reported in 2 stigma (Table 2). The median value of the calendar age curve was used as an estimate of calendar age.

The $\delta^{13}C$ corrected radiocarbon ages from CAIS were then entered into CLAM 2.2 (Blaauw, 2010) in order to generate three age models for the core. Three age models were necessary to represent the rapid and slow accumulation rates of sediment within three distinctly different depositional environments, which include: an active deep spring/wetland, a less active wetland and a deep perennial lake. The top 20 cm of the core were modeled using linear interpolation, with a goodness fit equal to 1.64 (Fig. 5). Linear interpolation was the best choice due to the high sedimentation rates of the spring. The second age model for 20–49 cm of the core was based on polynomial regression, with a third-order smoother, and a goodness fit equal to 768.53 (Fig. 6). Polynomial regression was the preferred choice for this portion of the core due to changing sedimentation rates as the site transitioned from an active spring/wetland to deeper, less active wetland deposits. Additionally, this age model was chosen for the ability to estimate the uncertainty between sample 41 cm, with a $\delta^{13}C$ corrected radiocarbon age of 1610±22 radiocarbon years before present (^{14}C yr BP) and sample 44 cm, with a $\delta^{13}C$ corrected radiocarbon age of 2991 ±25 ^{14}C yr BP. The third age model used a smoothing spline, with a smoother of 0.45, and a goodness fit equal to 672.65 to estimate the ages from 49–382 cm (Fig. 7). The smoothing spline best captured the estimated ages for the rapid deposition of samples 59, 70, and 80 cm, and showed the best ability to incorporate the depositional hiatus of the wetland between approximately ~ 5.8 and 7.1 cal ka BP.

Four age reversals were removed as outliers from the third age model. Of the four age reversals, samples 90 cm and 118 cm had $\delta^{13}C$ corrected radiocarbon ages of 12311 ±130 ^{14}C yr BP and 13148 ±55 ^{14}C yr BP, respectively. These two dates were removed from the age model due to the mixing of lake sediment as Lake Bonneville dropped

rapidly from the Provo level and regressed to altitudes of 1280 masl, eventually splitting into Lake Gilbert in the Great Salt Lake basin and Lake Gunnison in the Sevier basin by 13 cal ka BP (Goebel et al., 2011). During the Younger Dryas, Lake Gilbert (located to the north of the NRS14A study site) then transgressed to approximately 1300 masl, and eventually regressed to elevations below 1287 masl by ~11.0–10.2 cal ka BP. These rapid regressive/transgressive phases in lake levels most likely caused older carbon to be deposited on top of younger carbon as sediment slumped/eroded back into the basin (Oviatt, 2015), resulting in age reversals.

The third age reversal occurred in sample 242 cm, with a $\delta^{13}C$ corrected radiocarbon age of 19002 ±60 ^{14}C yr BP and can be attributed to the Bonneville flood. The Bonneville flood occurred at approximately 18 cal ka BP, and consequently reworked the sediment during this time to result in the mixing of older carbon with younger carbon. Finally, sample 379 cm, with a $\delta^{13}C$ corrected radiocarbon age of 18586 ±70 ^{14}C yr BP, represents the fourth age reversal. This age reversal is most likely the result of younger carbon, such as woody material, from the surface being dragged down during extraction of the sediment core. With the removal of these four dates, interpolation to the bottom of the core suggests the NRS14A record represents the last ~36.8 cal ka B.P. Table 2 presents the chronological framework of NRS14A.

Magnetic Susceptibility

Samples were removed at 1-cm increments and placed into 8-cc-volume cups for Magnetic Susceptibility analysis. The analysis was measured in standard international (SI) units using a Bartington *MS2* Magnetic Susceptibility System. Magnetic

Susceptibility measures the ease with which sediments take a charge. The susceptibility of sediments to magnetization increases with the amount of iron-bearing sediments present in the sample (Zolitschka et al., 2001). Iron-bearing clastic sediments are transported into the basin from terrestrial sources by surface runoff and thus are used as a proxy for erosional and flood events, as well as large-scale disturbances, such as fire and volcanic eruptions. Magnetic susceptibility data were graphed on a log base-10 scale to visualize the small magnitude changes in values over the record.

Loss on Ignition

One-cc-volume subsamples were taken at 4-cm increments of the sediment core and placed into ceramic cups for loss-on-ignition analysis (LOI). The samples were subsequently placed in an oven and dried at 100^{o}C, then burned at 550^{o}C and 900^{o}C in order to burn off water, organic matter, and carbonate, respectively. The loss-on-ignition method was described by Dean (1974) to determine the percent of water, organic, and carbonate content of sediments. In closed-basin lacustrine sediment, the percentage of carbonate is a sensitive proxy for lake level change, as well as for variations in temperature and humidity (Bischoff et al., 1997; Patrickson et al., 2010; Wetzel, 2001). Oviatt (1997), for example, found an inverse correlation between percentage calcium carbonate and lake levels during Lake Bonneville's transgressive phase.

Charcoal

Charcoal analysis is one of the few methods used in reconstructing fire histories of treeless landscapes, due to the absence of tree-ring and fire-scar proxies (Mensing et

al., 2006). In order to provide a fire history record for this shrub-dominated environment, macroscopic charcoal analysis was completed at contiguous 1-cm increments throughout the core. Samples of 5 to 10-cc were taken from the 8-cc magnetic susceptibility cups and placed in whirl-pack bags. The samples were then soaked for at least 24 hours in sodium hexametaphosphate to disaggregate the sediments, and then washed through 125-µm and 250-µm nested sieves of mesh. These sieve sizes were selected based on previous studies that determined charcoal size fractions >250-µm do not travel far from their source and thus represent local (watershed) fire events, while charcoal size fractions <125-µm represent regional fire events (Clark 1988; Gardner & Whitlock 2001; Whitlock & Millspaugh 1996). Following sieving, the remaining material was transferred to gridded petri dishes in order to identify and count charcoal particles under a dissecting microscope at ~20–40X magnification. Charcoal values were graphed on a log-base-10 scale to visualize the small- magnitude changes in values over the record.

The total charcoal counts were converted into charcoal concentrations (CHAR particles/cm²) and then calculated into charcoal influx (particles/cm^2/yr) using a statistical treatment program, Char Analysis. Char Analysis determines the timing of fire events and estimates past fire return intervals (FRI), as well as peak-detection to reconstruct a local fire history (Higuera, et al., 2009; Huerta, et al., 2009). Two components were used to graph CHAR, including a varying background which represents fluctuations in fire activities, and the peaks which indicate local fire episodes. The background was calculated by using a 1500- year lowess smoother. The fire return interval (FRI) is the number of years between each fire episode. However, the FRI has been excluded due to the poor depositional characteristics associated the large Pleistocene lake, as well as the

treeless, desert landscape of the study site inferring with the FRI. Fire episode magnitude or peak magnitude (particles/cm²/episode) indicates the amount of charcoal generated at each fire episode and varies with fire size, severity, and proximity (Higuera, et al., 2009).

Pollen

Pollen analysis was completed for the North Redden core to establish a record of the local and regional vegetation change over time at a ~500-year resolution. One cubic centimeter was processed at 6-cm intervals the upper 33-cm of the core and two cubic centimeters for 38–48 cm of the core. One cubic centimeter was processed at 10-cm intervals for samples 50–290 cm. Two cubic centimeters were then processed at 10-cm intervals from 290–380 cm. Pollen processing followed the standard palynological methods from Faegri et al. (1989). The spore *Lycopodium* was added to each sample as an exotic tracer to calculate pollen concentration and accumulation rates. Pollen samples were mounted on glass slides with silicone oil and examined under a light microscope at 500x magnification. In order to calculate influx rates and identify changes in the vegetation composition over time, each sample had a minimum of 300 identifiable terrestrial pollen grains, or 300 *Lycopodium* counted per sample.

The pollen data were then input into Tilia software to generate the percentages of total pollen based on the abundance of each pollen type, relative to the sum of terrestrial grains in each sample. Taxa with low counts were exaggerated by a factor of five on the pollen diagram. Additionally, the pollen percentage data are presented as zonal averages using CONISS (Grimm, 1987). For the purposes of this study, these zonal boundaries were used to describe the depositional and disturbance history, as well as the vegetation

and climate history of North Redden Springs.

Furthermore, the pollen influx data were analyzed using pollen ratios to identify climatic and vegetation regime changes through time. The ratio of *Artemisia* to Amaranthaceae pollen (calculated by *Artemisia* – Amaranthaceae) / (*Artemisia* + Amaranthaceae)) can be used to track moisture over time; higher abundances of *Artemisia* indicate relatively mesic periods, while increases in Amaranthaceae indicate a relatively xeric climate (Mehringer, 1985; Wigand, 1987; Mensing et al., 2004). Likewise, the ratio of Amaranthaceae + *Artemisia* to conifer pollen (calculated by *Artemisia* + Amaranthaceae – *Pinus*+*Abies*+*Picea*) / (*Artemisia* + Amaranthaceae + *Pinus*+*Abies*+*Picea*)) signals the existence of a dry shrub steppe (more Amaranthaceae + *Artemisia*) at 19, 15.5, and at 14 cal ka BP to present and the presence of a pine forest (more *Pinus, Abies, Picea*) at 34, 18, and 15 cal ka BP. Louderback and Rhode (2009) interpret increases in Amaranthaceae pollen and concurrent decreases in conifer pollen from the Blue Lake core as indicators of warmth and drying. Additional climate transitions can be identified through the ratio of *Pinus* to Cupressaceae pollen (calculated by *Pinus* – Cupressaceae) / *Pinus* + Cupressaceae)), which have been used by Louderback and Rhode (2009) to interpret a cooler/wetter climate when the ratio of *Pinus* is higher and a warmer/drier climate when the ratio of Cupressaceae is higher. Finally, the ratio of Poaceae to Amaranthaceae pollen (calculated by Poaceae –Amaranthaceae) / (Poaceae + Amaranthaceae)) has been used by Eckerle et al. (2013) as a measure of winter moisture and is based upon the gradient of more grass mixed with sage in the Pacific Northwest than in the area to the southeast. Winter insolation is also plotted

alongside the ratio of Poaceae (more winter moisture) to Amaranthaceae (less winter moisture) pollen to determine the timing of warmer winters.

Table 2
AMS Radiocarbon Dates

Site	UGAMS #	Depth (cm)	Radiocarbon Age	$\delta^{13}C$	Cal yr BP (CALIB)
NRS14A	18463	19-20 cm	-885 ±24	-26.5	-38
NRS14A	19178	27-28 cm	218 ±21	-25.3	270-304
NRS14A	A20060	35-36 cm	2152 ±22	-25.9	2060-2161
NRS14A	17942	40-41 cm	1610 ±22	-25.6	1415-1554
NRS14A	19179	43-44 cm	2991 ±25	-24.8	3312-3317
NRS14A	A20061	47-48 cm	4174 ±23	-25.9	4622-4764
NRS14A	A20727	48-49 cm	5543± 29	-23.7	6292 - 6397
NRS14A	18464	49-50 cm	6407 ±33	-23.0	7273-7418
NRS14A	17943	58-59 cm	6869 ±35	-23.1	7650-7788
NRS14A	A20062	69-70 cm	6798 ±124	-27.6	7456-7865
NRS14A	19180	79-80 cm	6642 ±30	-25.5	7470-7576
NRS14A	A20063	89-90 cm	12311 ±130	-22.6	13921-14989
NRS14A	19181	99-100 cm	10901 ±40	-24.6	12701-12827
NRS14A	18465	117-118 cm	13148 ±55	-23.2	15578-16020
NRS14A	18466	135-136 cm	11863 ±46	-24.2	13567-13767
NRS14A	18467	207-208 cm	11952 ±43	-25.0	13702-13990
NRS14A	18468	223-224 cm	13990 ±54	-22.5	16714-17210
NRS14A	19182	241-242 cm	19002 ±60	-20.0	22621-23105
NRS14A	18469	252-253 cm	17088 ±57	-22.8	20426-20821
NRS14A	17944	291-292 cm	17175 ±48	-23.3	20541-20906
NRS14A	18470	331-332 cm	23232 ±85	-21.7	27315-27683
NRS14A	19183	349-350 cm	26772 ±90	-21.5	30754-31119
NRS14A	18471	378-379 cm	18586 ±70	-23.8	22311-22624

AMS radiocarbon dates for NRS14A reported in 2 Sigma. Ages were calibrated using CALIB 7.0 and 7.1. Red indicates an age reversal.

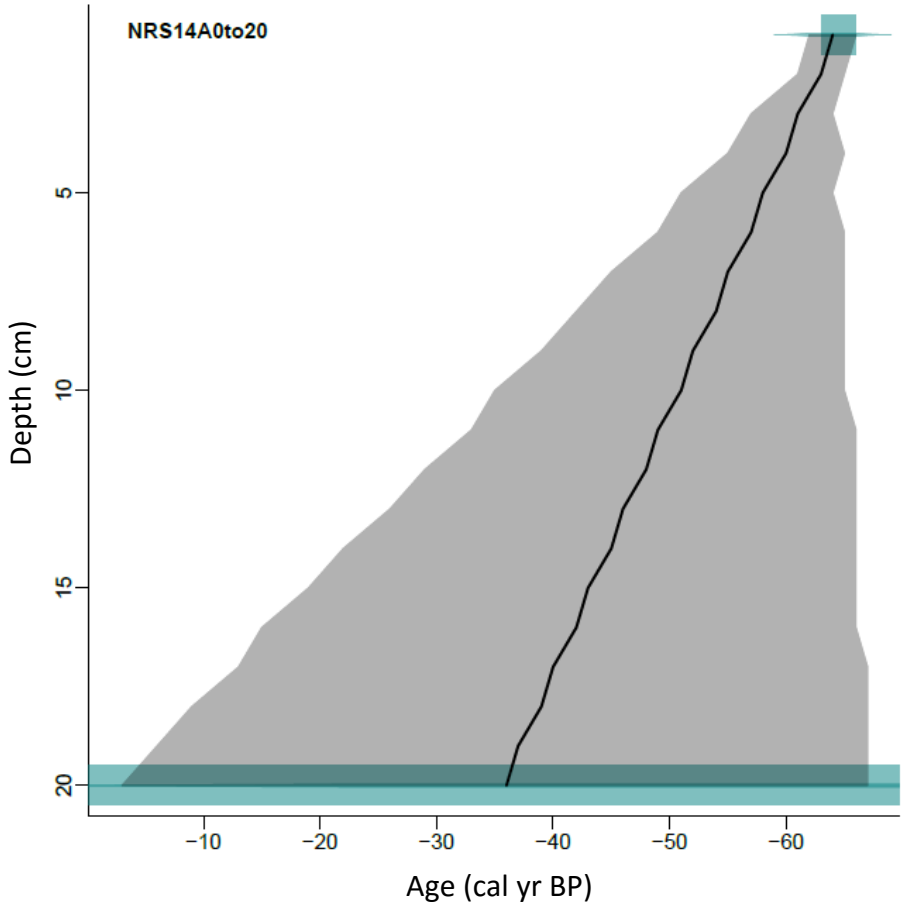

Figure 5. NRS14A age model for 0–20 cm based on linear interpolation. Blue indicates the calibrated radiocarbon date probability, beginning at -64 radiocarbon years. Gray shading indicates the 95% confidence interval for interpolated ages.

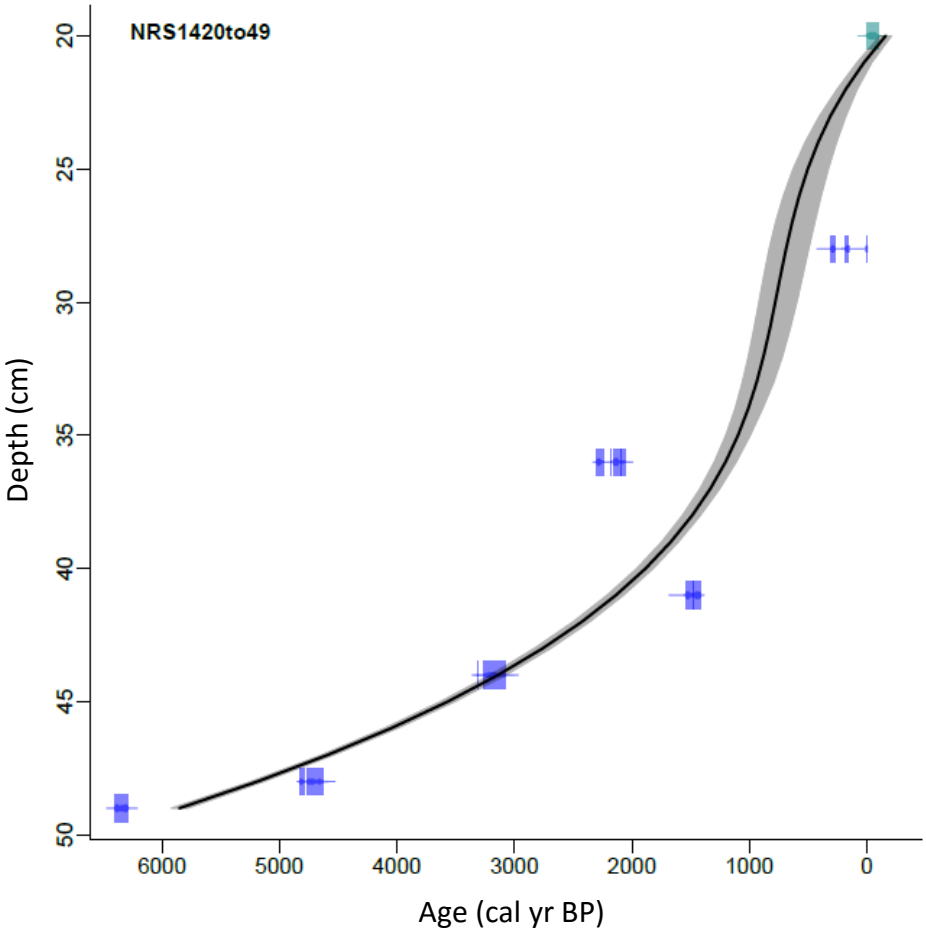

Figure 6. NRS14A age model for 20–49 cm based on polynomial regression. Blue indicates the calibrated radiocarbon date probability distributions. Gray shading indicates the 95% confidence interval for interpolated ages.

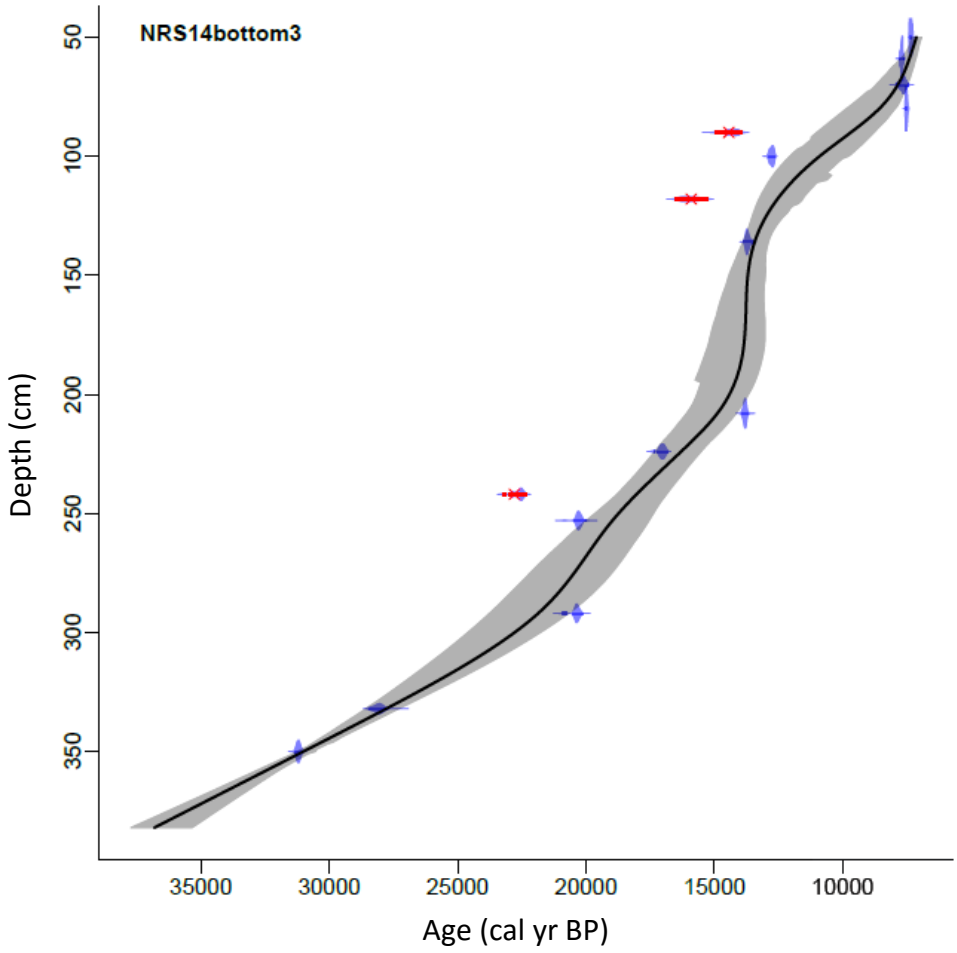

Figure 7. NRS14A age model for 49–382 cm based on smoothing spline. Blue indicates the calibrated radiocarbon date probability distributions. Red indicates dates removed as outliers from the age model. Gray shading indicates the 95% confidence interval for interpolated ages.

RESULTS

Pollen assemblages were divided into four zones based on CONISS results. Charcoal, loss-on-ignition, and magnetic susceptibility (MS) analyses are described according to each zonal boundary (NRS14A Zones I–IV) below. The radiocarbon chronology of the core is provided in a composite age model (Fig. 8).

Chronology

AMS radiocarbon dates for North Redden Springs are shown in Table 2. Ages were calibrated using CALIB 7.0 and 7.1 and reported as 2 sigma. Of the 23 radiocarbon dates, 4 represent age reversals that are not in stratigraphic order. These reversals are likely a result of a combination of factors, including: mixing of sediments as lake levels regressed rapidly from the Provo level to eventually the Gilbert level during the Younger Dryas; mixing of sediments following the Bonneville flood; and younger carbon from the surface being dragged down during extraction of the sediment core. The age reversals, as well as the calibrated dates and the depositional hiatus of the wetland (~5.8–7.1 cal ka BP), are shown in the composite age model (Fig. 8).

NRS14A Zone I: Late Pleistocene *Artemisia* Steppe/Lake Bonneville (Depth 382–339 cm, 36.8–29 cal ka BP)

Depositional and Disturbance History

The stratigraphy of NRS14A zone I consist of greenish-gray clay, with thin (~1-millimeter wide; ~1-millimeter apart) laminae of white clay (see Appendix). These laminae (likely seasonal varves) are present from 36.8–31.3 cal ka BP. Laminae are not present from ~ 31.3–30.8 cal ka BP. Beginning at 30.8–27.7 cal ka BP, the spacing in-between the thin white lamiae transitions to 1 centimeter. The clay composition of the sediment corresponds to high values of percent carbonate that vary (~31–11 %) throughout this period (Fig. 9). Magnetic susceptibility (MS) values vary from less than one to six SI, with a decrease below one SI occurring at 32.2 cal ka BP. Percent carbonate increases to ~31% at this time. Low charcoal values and no fire events occur during NRS14A zone I (Fig. 10).

Vegetation and Climate History

The dominant vegetation of NRS14A zone I consist of *Artemisia* (30–50%) and *Pinus* (25–40%), with 10% identified as *Pinus*-haploxylon-type consistent with *Pinus flexilis* (Fig. 11). Both *Picea* and Amaranthaceae pollen were less than 5% of terrestrial pollen. Herbaceous pollen, such as Asteraceae, was common at 5%. Other vegetation types included rose and *Ambrosia.*

Pollen ratios were calculated based on pollen influx data. The average ratio of *Artemisia* to Amaranthaceae (wet/dry climate index) is -0.49, as indicated by the red line in Figure 12. Throughout NRS14A zone I, the ratio of *Artemisia* (wet) to Amaranthaceae (dry) pollen exceeded the average towards higher values of *Artemisia*. Pollen ratios were

also calculated for conifers (*Pinus, Picea,* and *Abies*) to *Artemisia* + Amaranthaceae, with an average ratio of 0.25 (Fig. 13). A higher ratio of *Artemisia* + Amaranthaceae pollen indicate a dry shrub steppe, while a higher ratio of conifer pollen signals a wet pine forest. The ratio of *Artemisia* + Amaranthaceae exceeds the ratio of conifer pollen during this period, until 34 cal ka BP. Additionally, the ratio of *Pinus* pollen (wet climate) to Cupressaceae pollen (dry climate) transitions towards higher values of *Pinus*, with an average ratio of 0.43 (Fig. 14).

The ratio of Amaranthaceae (less winter moisture) to Poaceae (more winter moisture) pollen is plotted alongside December insolation (W/m^2) for 30°N latitude (Fig. 15). The average ratio of Amaranthaceae to Poaceae is -0.49 and is indicated by the red line within the figure. Throughout NRS14A zone I, the ratio of Amaranthaceae was higher and shifting towards more Poaceae. December insolation values were low (~218 W/m^2) and gradually increasing.

Lastly, charcoal ($particles/cm^3/yr$), total influx pollen and the ratio of *Artemisia* (wet climate) to Amaranthaceae (dry climate) is plotted in Figure 16. Charcoal values mirror total influx pollen for most of the record, until 29 cal ka BP, when pollen influx values increase.

NRS14A Zone II: Latest Pleistocene Conifer Forest/ Lake Bonneville

(Depth 339–221 cm, 29–16 cal ka BP)

Depositional and Disturbance History

In NRS14A zone II, the sediment consists of greenish-gray clay with thin (~1-millimeter wide; ~1-centimeter apart) white laminae (see Appendix). Beginning at 27.5 and spanning to 21.8 cal ka BP, the laminae become wider (~2-centimeters wide). Coarse

gray bands are present at 21.4 cal ka BP and at 20.6 cal ka BP. The sediment transitions to greenish-gray clay beginning at 20.5 to 18.9 cal ka BP. A coarse gray band occurs at 18.9–18.8 cal ka BP. Sediment then shifts to gray, sticky clay with deposits from 18.8–18.3 cal ka BP. A 1-centimeter-wide band of course, dark gray sediment occurs from 18.3–18.1 cal ka BP. Sediment then transitions back to gray, sticky clay beginning at 18.1 to 15.1 cal ka BP.

Throughout NRS14A zone II, the percent carbonate fluctuates between ~12% to ~22% from 29 to 22 cal ka BP, with a slight increase to ~19% at 21 cal ka BP (Fig. 9). MS values decrease (~0.8 SI) in parallel to a decrease in percent carbonate to ~14% at 27 cal ka BP. MS values decrease to 0.7 SI once again, while the percent of carbonate increases to ~23% at ~25 cal ka BP. MS values then continue to vary throughout the record, until a decrease to ~5.5 SI occurs at 18 cal ka BP. The percent carbonate values at 18 cal ka BP increase to ~20%, and subsequently decreased to ~15%. This decrease in percent carbonate is followed by an increase in MS to ~62 SI at 16.6 cal ka BP. Charcoal values remain low during NRS14A zone II, with the exception of one fire episode identified at 21 cal ka BP, with a peak magnitude of 0.2 particles/cm^2/episode (Fig. 10).

Vegetation and Climate History

The zonal pollen percentage averages for arboreal species, *Pinus* (80%), *Abies* (10–25%), and *Picea* (5%), increased during NRS14A zone II (Fig. 11). Of the *Pinus* pollen percentages, 5–10% consisted of *Pinus*-haploxylon-type. *Artemisia* and Asteraceae pollen percentages decreased to below 5%, and *Ambrosia* fell to 0%. Amaranthaceae pollen percentages varied from 0 to ~20% and increased to 60% at 19 cal ka BP, with a

subsequent decrease. Poaceae had a zonal average of 5–25%, and *Botryococcus* pollen percentages increased to 30% during this period.

The ratio of *Artemisia* to Amaranthaceae pollen deviated from the average, with two distinct shifts towards more Amaranthaceae pollen at ~21.5 cal ka BP and at ~19 cal ka BP (Fig. 12). A similar pattern occurs in the ratio of conifer to *Artemisia* + Amaranthaceae pollen at ~19 cal ka BP, when the ratio of *Artemisia* + Amaranthaceae pollen exceeded the average (Fig. 13). However, for the most part, NRS14A zone II is identified as having high relative abundance of conifer pollen (Fig. 14).

Comparable patterns can also be found in the ratios of Amaranthaceae to Poaceae pollen and December insolation (W/m^2) for 30°N (Fig. 15). The ratio deviates from the average towards more Amaranthaceae at ~22 cal ka BP and at ~19 cal ka BP. Additionally, the ratio shifts to more Poaceae at 22 cal ka BP and at 19 cal ka BP, with relatively high December insolation values at this time.

NRS14A Zone III: Early and Middle Holocene Xeric Shrub/ Lake Bonneville-Wetland (Depth 221–49 cm, 16–6.0 cal ka BP)

Depositional and Disturbance History

Sediments from NRS14A zone III were composed of gray clay that shifted to light greenish-gray clay from 15 to 13.4 cal ka BP (see Appendix). Sandy, dark gray bands are present: 13.9, 13.8, 13.7, and 13.75 cal ka BP. Swift transition occurs at 13.4–12.6 cal ka BP to extremely gritty, gray sediment interspersed with tufa deposits. From 12.6 to 7.4 cal ka BP, sediments consisted of pale green clay/marl. A darker gray band occurs at 7.4–7.3 cal ka BP. Sediments from 7.3 to 5.8 cal ka BP consist of loamy/chalky greenish gray

marl.

The percent carbonate values for NRS14A zone III increases to 23% at ~15 cal ka BP, with a spike occurring at 14.5 cal ka BP, and a decrease (14%) by ~13 cal ka BP (Fig. 9). Percent carbonate values fluctuate between ~10–16% throughout NRS14A zone III. MS values vary between 3–20 SI. Increases in charcoal values occur at 13.8 (0.3 particle/cm²/yr), 11.8 (0.5 particle/cm²/yr), and at 7.5 (0.7 particle/cm²/yr). Fire episodes were identified at 15, 12, 11.5, 7.5, and 6 cal ka BP (Fig. 10). Peak magnitudes varied from 0 to 20.0 (particles/cm²/episode).

Vegetation and Climate History

The zonal average for arboreal pollen percentages of *Pinus* (0–25%), *Abies* (0–5%), and *Picea* (0–5%) decreased during NRS14A zone III (Fig. 11). Beginning at 14 cal ka BP, the average pollen percentages of *Populus* (10%), Cupressaceae (5–10%), *Quercus* (5%), Rose (<5%), *Sarcobatus* (5%), Asteraceae (< 5%), Cyperaceae (10%), and *Botryococcus* (45%) increased. Pollen percentages of Amaranthaceae also increased beginning at 16 cal ka BP and varied between 10–60% throughout the period. The percent of aquatics signals the presence of the wetland. Additionally, at 15 cal ka BP, Poaceae pollen percentages increased and varied from 5 to 40%. Apiaceae cf *P. bolanderi* varied at 15% at 16 cal ka BP.

In NRS14A zone III, the ratio of *Artemisia* to Amaranthaceae pollen abruptly (within ~1000 years) shifted towards more Amaranthaceae at 15 cal ka BP, and subsequently towards more Artemisia at 14.5 cal ka BP (Fig. 12). More Amaranthaceae pollen is present from 14 cal ka BP to the end of the period at 6 cal ka BP.

Three changes were identified in the ratio of conifers to *Artemisia* + Amaranthaceae pollen: a shift towards more dryland shrubs at 15.5 cal ka BP, a shift towards more conifers at 14.5 cal ka BP, and lastly, more dryland shrubs from 14 cal ka BP to the end of the period at 6 cal ka BP (Fig. 13).

The ratio of Cupressaceae to *Pinus* pollen deviates from the average towards more Cupressaceae during NRS14A zone III, with a notable transition to *Pinus* at 14 cal ka BP and at 13 cal ka BP (Fig. 14). Additionally, the ratio of Amaranthaceae to Poaceae pollen indicates more Amaranthaceae pollen during the first part of the zone, with a transition to more Poaceae at 14.5 cal ka BP (Fig. 15). The remainder of the zone consists of more Amaranthaceae, which parallels decreasing values of December insolation.

NRS14A Zone IV: Late Holocene Xeric Shrub/Wetland-Spring

(Depth 49–0 cm, 6.0 cal ka BP–Present)

Depositional and Disturbance History

NRS14A zone IV consists of greenish gray, loamy marl from 5.8 to 2.7 cal ka BP (see Appendix). From 2.7 cal ka BP to AD 1989, the sediment transitioned to dark gray/brown loamy clay, with areas of sandy/silt. The sediment from AD 1989 to present consisted of brownish/black wetland deposits. A dense root mat makes up the deposits dating from AD 1995 to present.

The percent carbonate of NRS14A IV averages ~14% at the start of the period, and is followed by a decrease to ~2% beginning at 5.5 to 1.0 cal ka BP (950 AD) (Fig. 9). Percent carbonate values then increased (~15%) at 1.0, until values decreased (~3%) at 150 cal ka BP to present. The percent organics increase in a similar pattern (~2 to <

20%), beginning at 1.0 cal ka BP to present. MS values averaged at 8 SI for most of the period, however, an increase (30 SI) occurred at 1.0 cal yr BP. Historical MS values averaged ~7–13 SI. Charcoal values began increasing from 4.0 cal ka BP to present (Fig. 9). Three fire episodes were identified at 6; 3.8, and 2.5 cal ka BP, with peak magnitudes of 0.5, 0, and 0.2 (particles/cm/ep), respectively (Fig. 10).

Vegetation and Climate History

The zonal average pollen percentages for xeric shrubs, Amaranthaceae, increased from the previous zone and varied from 50 to 80% (Fig. 11) throughout NRS14A zone IV. The zonal percentage averages for arboreal pollen also increased, and included *Pinus* (10%), *Abies* (5%), *Picea* (<5%), and *Populus* (20%). Overall, pollen percentages for trees, shrubs and herbs began increasing at ~1.0 cal ka BP (AD 950), and include Cupressaceae, *Quercus*, and Eleagnaceae cf *Elaeagnus angustifolia, Ambrosia*, Rosaceae, *Sarcobatus*, Asteraceae and Poaceae. Percentages of the aquatic *Botryococcus* varied from 50 to 5% throughout NRS14 zone IV. Average percentages of other aquatics, such as Cyperaceae, varied from 5 to 10% and follow the same pattern of increasing during the modern period (at ~1.0 cal ka BP).

The ratio of *Artemisia* to Amaranthaceae pollen deviates from the average towards more Amaranthaceae pollen for NRS14A zone IV (Fig. 12). Similarly, the ratio of conifers to *Artemisia* + Amaranthaceae pollen identifies more *Artemisia* + Amaranthaceae pollen present in this zone (Fig. 13). When the ratio of Cupressaceae to *Pinus* pollen is examined, the ratio crosses the average towards more *Pinus* between 6.0 and 2.0 cal ka BP (Fig. 14). From 2.0 cal ka BP to 150 cal BP (AD 1880), the ratio shifts

to more *Pinus* pollen, with abrupt shifts to more Cupressaceae and back to *Pinus* at the end of the record. Lastly, the ratio of Amaranthaceae to Poaceae (Fig. 15) indicate more Amaranthaceae, until the ratio deviates from the average towards more Poaceae at the end of the record. December insolation (W/m^2) for NRS14A zone IV begins increasing at 6 cal ka BP.

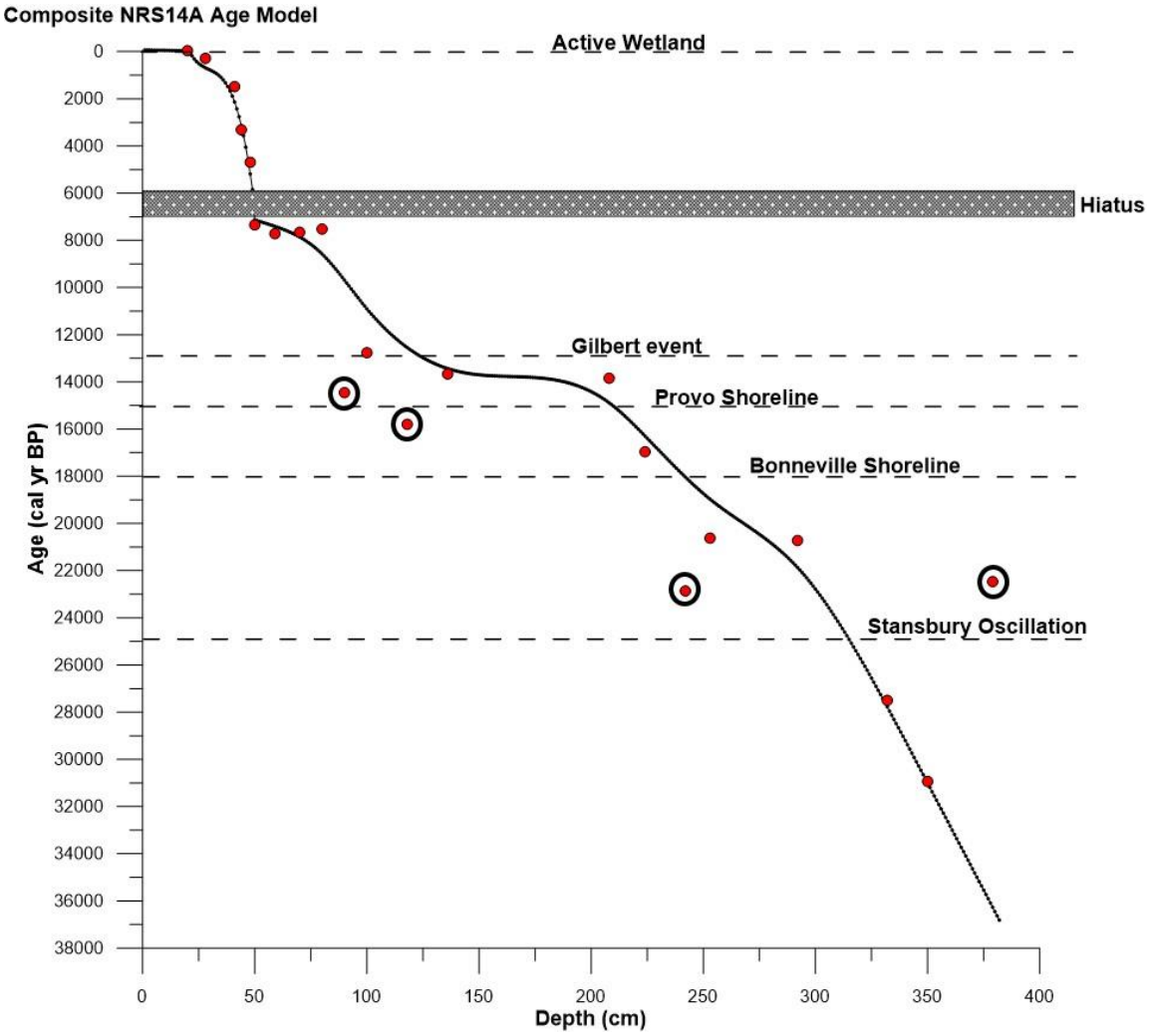

Figure 8. Composite Age Model. Line represents a composite of the three age models created using CLAM 2.2. Red dots indicate calibrated radiocarbon ages. The circled red dots indicate the age reversals not included in the models. The depositional hiatus (~5.8 to 7.1 cal ka BP) of the spring is shown in gray shading.

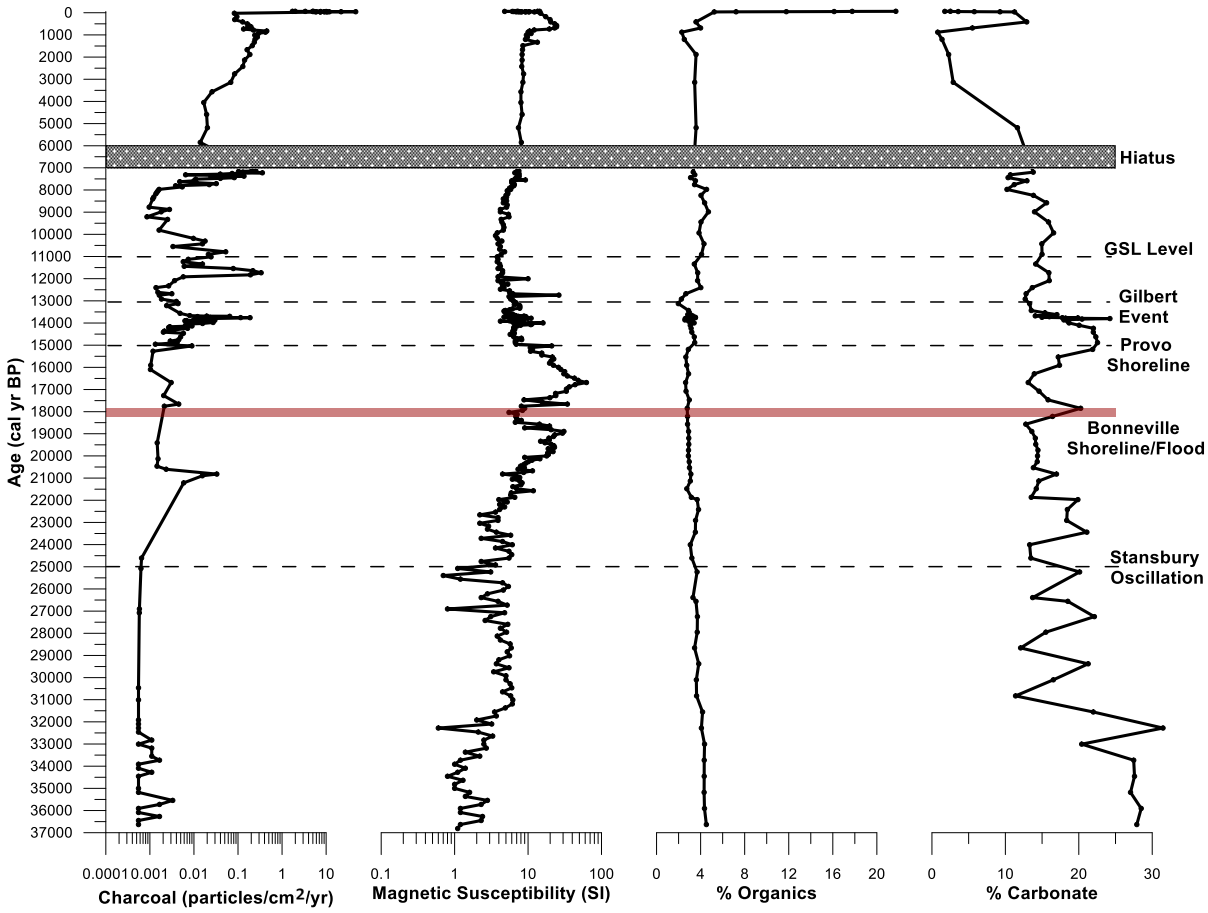

Figure 9. Charcoal, Magnetic Susceptibility and Loss-on-Ignition data. Grey indicates the depositional hiatus at the spring; Red indicates timing of Bonneville flood. Timings of known lake level events shown by dotted lines.

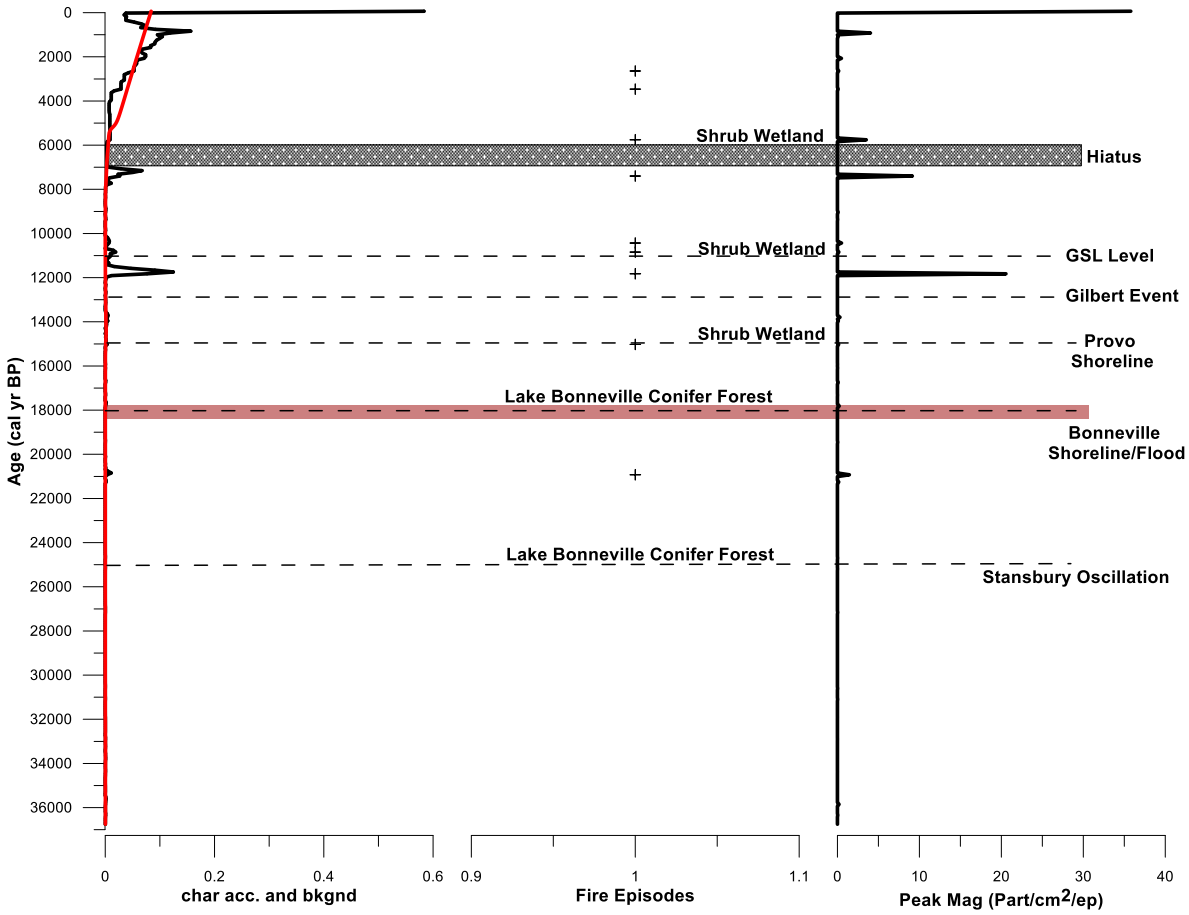

Figure 10. Fire history from CHAR Analysis data. Charcoal accumulation rates (CHAR) were smoothed using a moving window width of 1500 years (background-red line); fire episodes are indicated by "+" symbol when the CHAR exceeds the background. Peak magnitude (# particles/cm²/yr) indicates the magnitude of each peak detected. Grey bar indicates depositional the hiatus of the spring; Red-dotted bar indicates timing of Bonneville flood. Timing of known lake level events is shown by dotted lines. Dominant vegetation types from pollen are also provided.

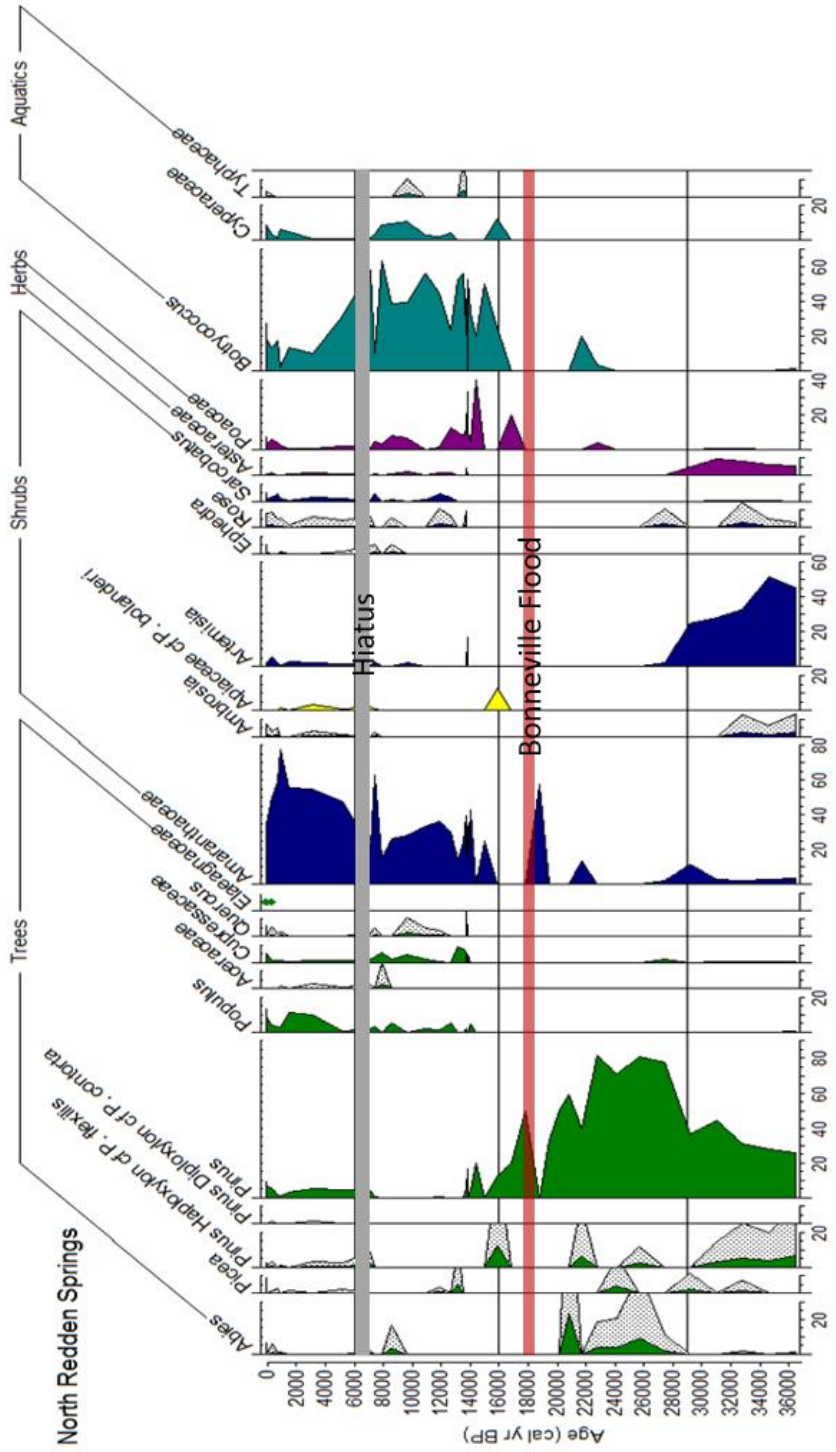

Figure 11. Percent Pollen diagram. Red shading indicates timing of Bonneville Flood. Grey bar indicates a depositional hiatus at the spring. Taxa with low counts have been exaggerated by a factor of 5x (gray shading).

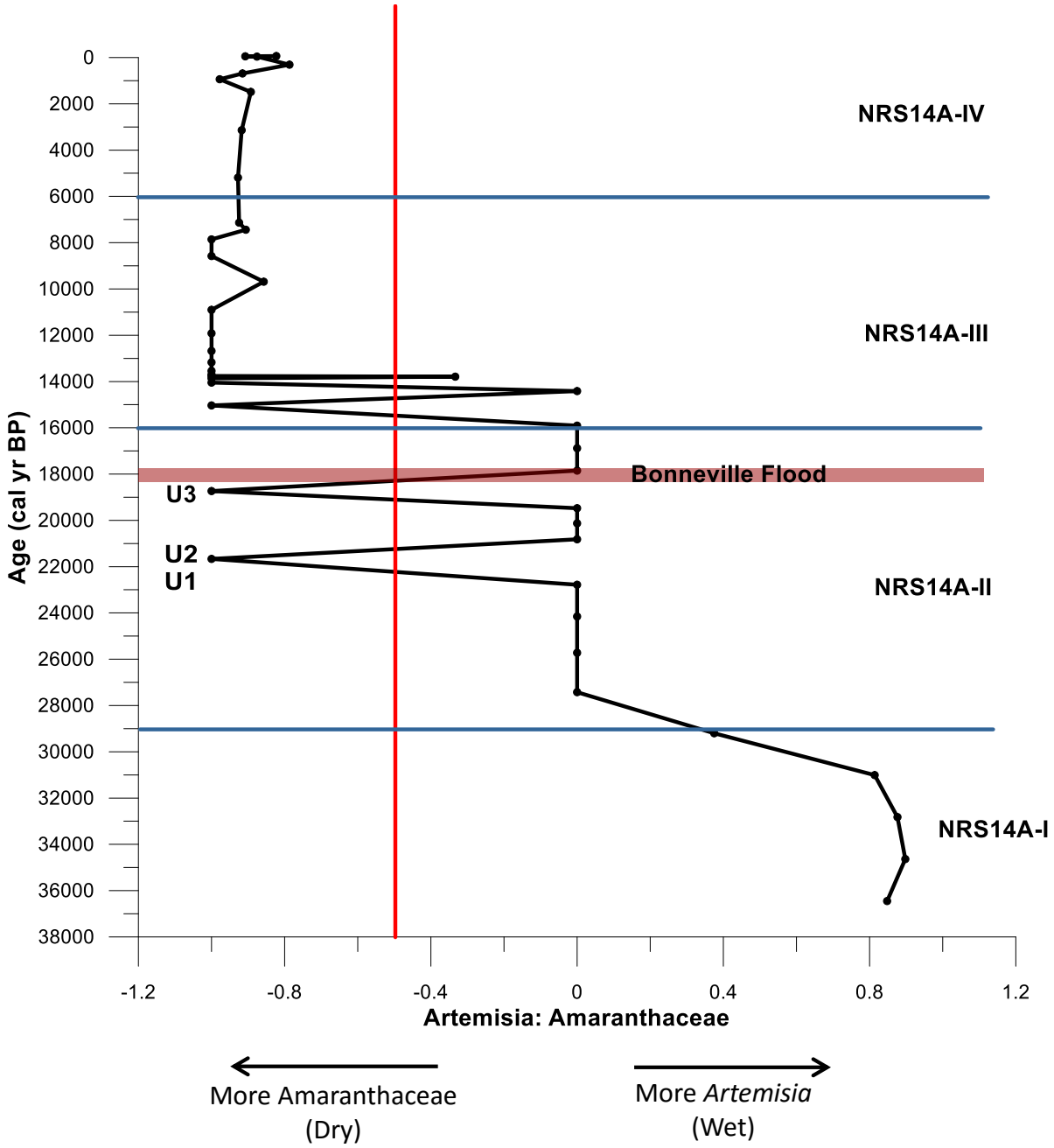

Figure 12. The ratio of Amaranthaceae to *Artemisia* pollen plotted over time. Red line indicates the average ratio (-0.49). Blue lines indicate zonal boundaries. Red shading indicates the timing of the Bonneville Flood. U1, U2, and U3 denote unnamed transgressive-phase oscillations. More Amaranthaceae pollen indicates dry climate conditions, while more *Artemisia* pollen indicates wet climate conditions.

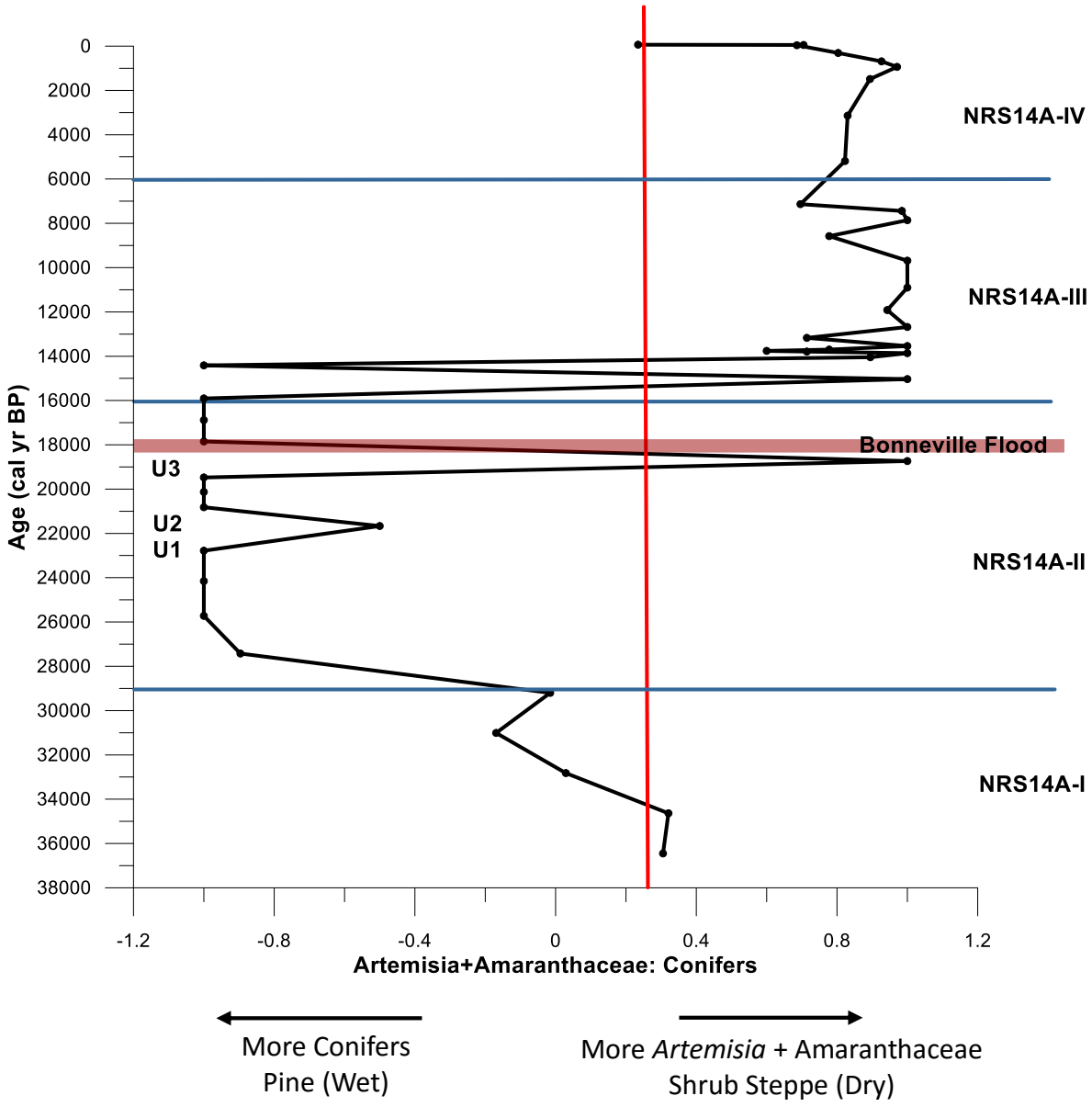

Figure 13. The ratio of Conifer to *Artemisia* + Amaranthaceae pollen plotted over time. Red line indicates the average ratio (0.25). Blue lines indicate zonal boundaries. Red shading indicates the timing of the Bonneville Flood. U1, U2, and U3 denote unnamed transgressive-phase oscillations. More conifer pollen indicates wet climate conditions, while more *Artemisia* + Amaranthaceae pollen indicates dry climate conditions.

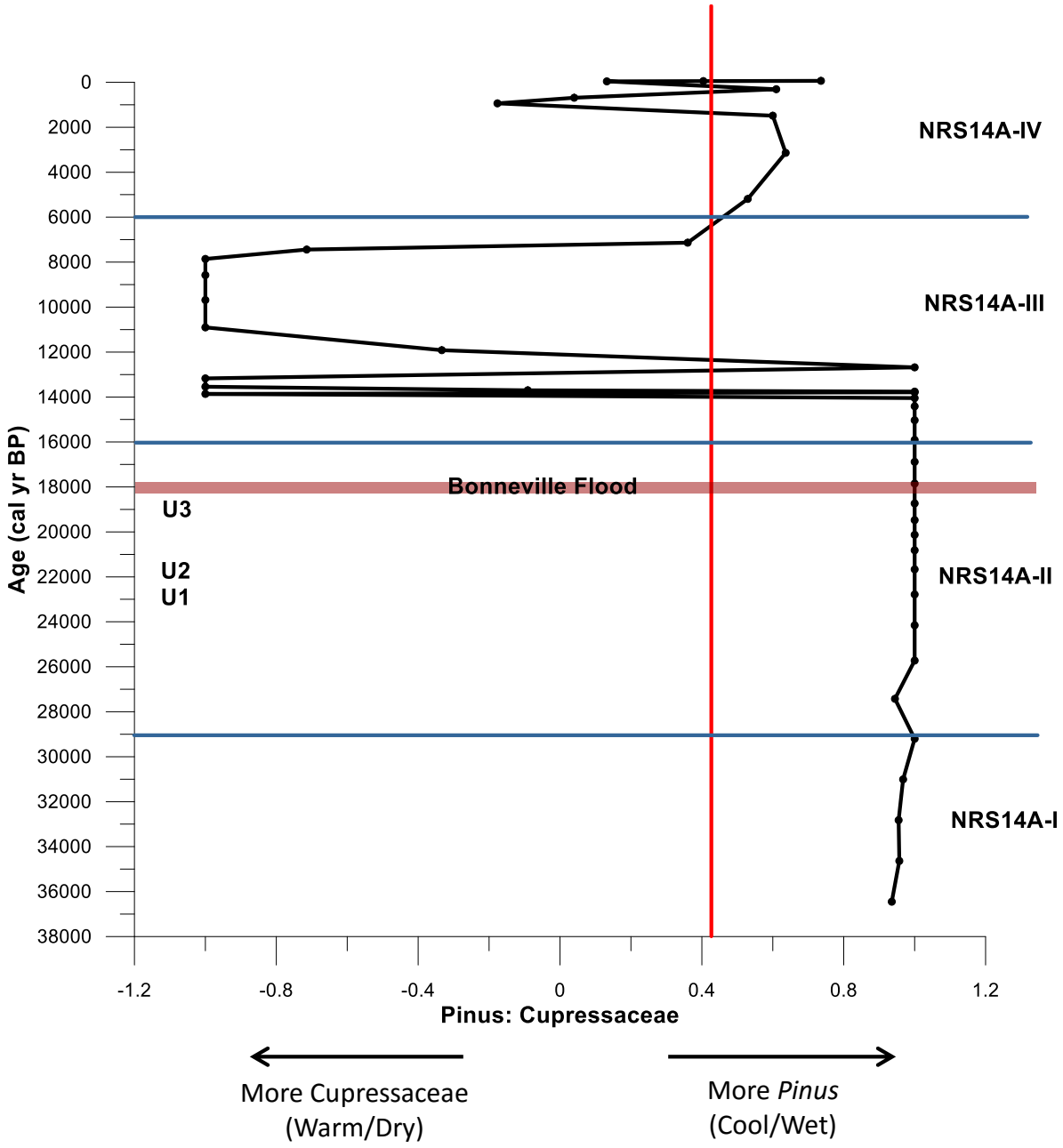

Figure 14. The ratio of Cupressaceae to *Pinus* pollen plotted over time. Red line indicates the total average ratio (0.43). Red shading indicates the timing of the Bonneville Flood. U1, U2, and U3 denote unnamed transgressive-phase oscillations. More Cupressaceae pollen indicates warm/dry climate conditions, while more *Pinus* pollen indicates cool/wet climate conditions.

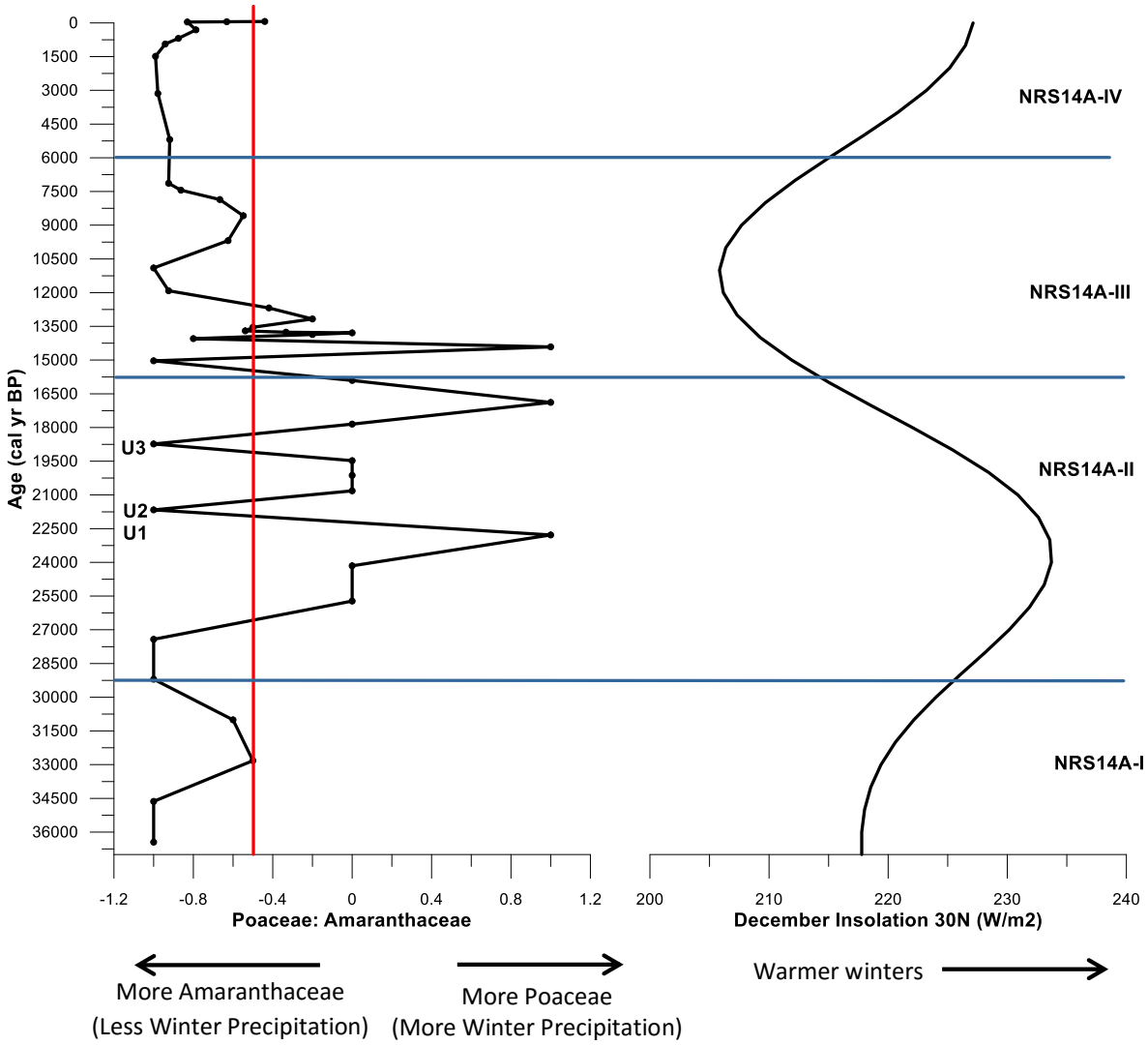

Figure 15. Comparison of the ratios of Amaranthaceae to Poaceae pollen and December insolation through time. Red line indicates the average ratio (-0.48). Blue lines indicate zonal boundaries. U1, U2, and U3 denote unnamed transgressive-phase oscillations. More Amaranthaceae pollen indicates less winter precipitation, while more Poaceae pollen indicates more winter precipitation. More winter insolation indicates warmer winters.

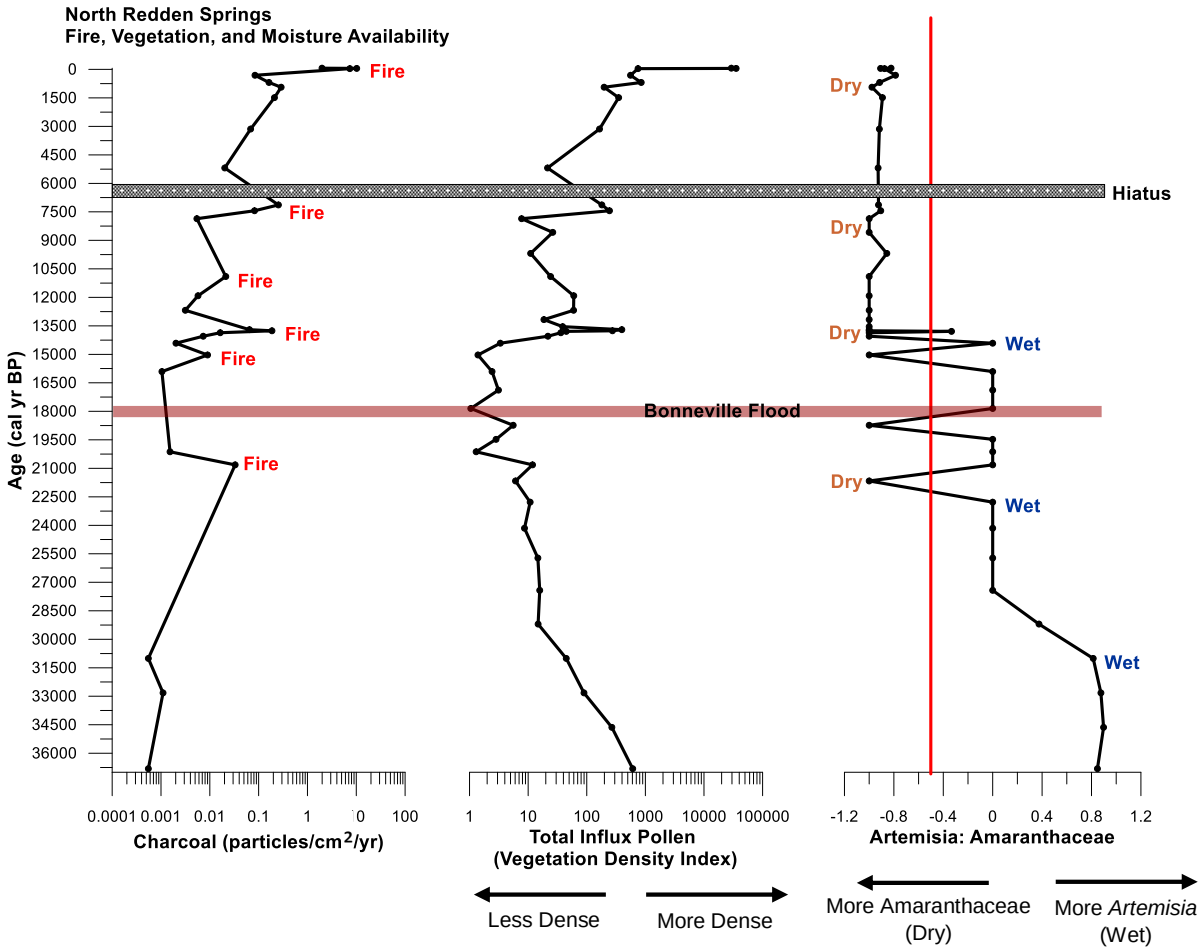

Figure 16. Comparison of charcoal data, total pollen influx (vegetation density index) and the ratio of *Artemisia* to Amaranthaceae pollen. Red line indicates the average ratio (-0.49). Grey shading indicates the depositional hiatus at the spring. Red shading indicates the timing of the Bonneville Flood. More Amaranthaceae pollen indicates dry climate conditions, while more *Artemisia* pollen indicates wet climate conditions.

DISCUSSION

A detailed reconstruction of environmental change for the Bonneville basin during the last 36.8 cal ka BP has been completed using AMS radiocarbon dating, pollen, macroscopic charcoal, magnetic susceptibility, and loss-on-ignition analyses. The objectives of this research have been met and include: (1) to describe the paleoenvironmental history of the last 36,800 years for the North Redden Springs Region of the Bonneville Basin, (2) to assess the paleoenvironmental data to refine the chronology of Lake Bonneville, and (3) to describe how the paleoenvironmental context may have impacted prehistoric human populations within the region. These objectives were chosen to better understand the chronology of climate change associated with Lake Bonneville as the study site transitioned from a large Pleistocene lake to a Holocene wetland. Also of interest is the impact these changes had on the depositional environment, and the impacts to disturbance and vegetation regimes. These changes are then related to prehistoric human populations within the basin.

For the purpose of this study, high values of magnetic susceptibility (MS) are used as a proxy to identify increased erosional input from terrestrial or volcanic sediment into the basin, while low MS values signify the removal of sediment out of the basin during a flood event. Percent carbonate values are interpreted as proxies for lake-level change and spring productivity; high percent carbonate values indicate lower lake-levels and more saline conditions. Conversely, low percent carbonate values indicate rising

lake-levels and freshwater conditions (Bischoff et al., 1997; Patrickson et al., 2010; Oviatt, 1997; Wetzel, 2001). Pollen percentages were used as a proxy to determine changes in local and regional vegetation over time. Pollen influx was used to calculate pollen ratios in order to determine vegetation density and fluctuations in the climate system. Lastly, sediments with greater charcoal content reflect an increase in the number of fire episodes. Findings are interpreted and discussed below in chronological order from oldest to youngest.

NRS14A Zone I: Late Pleistocene *Artemisia* Steppe/Lake Bonneville (Depth 382–339 cm, 36.8–29 cal ka BP)

Depositional and Disturbance History

The current understanding concerning the age at which Lake Bonneville formed is ~30 cal ka BP (Oviatt, 2015), when the upper Bear River was diverted after the Hansel Valley volcanic eruption (Reheis et al., 2014). However, the NRS14A lacustrine record, which extends to at least 36.8 cal ka BP, suggests that a lake may have existed in the Bonneville basin at a much earlier date. Accordingly, a shallow and warm-temperature lake existed at the study site during NRS14A zone I, as evident by the high percent carbonate values (~27%) and the laminae present in the sediment core from 36.8 to 31.3 cal ka BP (see Appendix). The laminae layers of white clay were most likely deposited during spring/summer months, while organic green clay layers were deposited during winter months.

The depositional lake environment of NRS14A zone I changed beginning at 33 to 32 cal ka BP, when percent carbonate and MS values oscillated (Fig. 9). These fluctuations represent the initiation of a transgressing and freshwater lake, as early as 33

cal ka BP, as evident by the decrease in percent carbonate (20%). Subsequently, at 32 cal ka BP, a concomitant decrease in MS values (0.6 SI), and an increase in percent carbonate values (31%) occurred, indicating lowering lake-levels, with an increase in the concentration of minerals. This possible regression event is documented as a deposit of uniform, greenish-gray sediment (absent of laminae) in the sediment core from 31.3 to 30.8 cal ka BP (see Appendix). However, lake levels returned to deep-water conditions by 30.8 cal ka BP, when percent carbonate values decreased to 11%, suggesting a rapidly rising lake at this time.

Beginning at 30.8 cal ka BP and lasting until 27.5 cal ka BP, the spring/summer organic deposits become wider (~1-centimeter wide) (Appendix), indicating a possible increase in spring/summer precipitation. Additionally, percent carbonate values increased (21%) and may reflect the large differences between water depths during winter months and spring/summer months. These depositional conditions correspond with "the summer monsoon hypothesis" proposed by Nishizawa et al. (2013), in which the Bonneville basin was dominated by increased spring/summer precipitation between ~50–28 cal ka BP (Lyle et al., 2012). The increased spring/summer precipitation from the tropical eastern Pacific and the Gulf of Mexico acted as a source of moisture, and thus can be interpreted as aiding in the formation of Lake Bonneville, sometime prior to 36.8 cal ka BP. Additionally, the increased spring/summer precipitation (from 38.8 to 27 cal ka BP) is shown in Figure 16.

Fires were infrequent during NRS14A zone I, with exceedingly low charcoal values and no fire episodes (Figs. 9, 10). The lack of charcoal at this time was in all likelihood the result of the inundation of the watershed by Pleistocene Lake Bonneville,

which may have also acted as a poor catchment for atmospheric charcoal particles.

Vegetation and Climate History

Cold and dry conditions existed at North Redden Springs prior to 29 cal ka BP, as evidenced by the presence of a desert shrub steppe consisting primarily of *Artemisia* and low-lying herbs and shrubs (Fig. 11). Arboreal conifer taxa, such as *Pinus*, *Picea,* and *Abies*, were most likely growing at higher elevations than modern. The North Redden pollen record of abundant *Artemisia* during the late Pleistocene is consistent with the regional pollen records older than ~24 cal ka BP from the Bonneville basin (Mehringer, 1985; Spencer et al., 1984; Thompson et al., 1992). These records display low values of *Pinus* and *Picea*, with high values of *Artemisia* and shrubs in the Amaranthaceae (e.g., shadscale, and saltbrush) and the Sarcobataceae (e.g., greasewood) families to thus indicate prevalent sagebrush-shadscale vegetation communities in valley bottoms, as *Pinus* and *Picea* developed in montane areas in these pre-24 ka deposits (Mehringer, 1985; Spencer et al., 1984; Thompson et al., 1992). Subsequent increases in *Pinus* and *Picea* pollen, along with the decline of *Artemisia* and Amaranthaceae pollen occurred as a possible response to deep-water conditions inundating shrub habitat. Taken together, these latest Pleistocene records demonstrate the presence of cold-adapted sagebrush steppe, with dispersed stands of spruce and pine in the cold, dry northern Bonneville basin, while the more mesic southern Bonneville basin supported a more diversified wood land-steppe mosaic dominated by bristlecone pine (Madsen, 2001).

Through the use of climate data obtained from NOAA National Climatic Data Center, it is possible to use pollen as a proxy for past vegetation in order to identify past

climate conditions. July temperatures for *Artemisia* must be within the range of 10–25 °Celsius, and January temperatures within -20–5 °Celsius. Additionally, *Artemisia* requires July precipitation to be between 5–80 mm and January precipitation between 5–100 mm, with an annual precipitation of 0–1000 mm (Williams et al., 2006). In general, high pollen percentages of *Artemisia* typically indicate winter cold and dry climates (Minckley et al., 2008). High *Artemisia* pollen percentages also indicate cold (but not the coldest) regions, with climate spaces that are intermediate between cool and warm regions and wet and dry regions (Minckley et al., 2008).

In addition, the ratios of Amaranthaceae to *Artemisia* pollen (Fig. 12), and of Cupressaceae to *Pinus* pollen (Fig. 14) demonstrate cooler and wetter conditions than present, due to a higher influx of *Artemisia* and *Pinus* pollen in NRS14A zone I. Moreover, the ratios of conifer to *Artemisia* + Amaranthaceae pollen further supports the presence of a shrub steppe growing at lower elevations than at present, with more *Artemisia* + Amaranthaceae pollen during NRS14A zone I, until ~34 cal ka BP (Fig. 13).

It can be concluded that during NRS14A zone I, the region received less winter precipitation, coincident with low values of December insolation (W/m^2) (Fig. 15), thus resulting in a desert shrub steppe at the study site. Diminished winter precipitation is consistent with the atmospheric-oceanic circulation mechanism, or "the summer monsoon hypothesis" proposed by Lyle et al. (2012). The Bonneville basin was most likely influenced by enhanced spring/summer precipitation from the tropical eastern Pacific and the Gulf of Mexico between ~50–28 cal ka BP (Nishizawa et al. 2013), until moisture sources began shifting at 28 cal ka BP to increase regional winter precipitation (Nishizawa et al., 2013). An increase in winter precipitation is reflected as an expanded

conifer forest and larger deposits of laminae in the following zone.

NRS14A Zone II: Latest Pleistocene Conifer Forest/ Lake Bonneville (Depth 339–221 cm, 29–16 cal ka BP)

Depositional and Disturbance History

Lake Bonneville began the transgressive phase and continued to deepen, with deposits of greenish-gray clay, and thin (~1-millimeter wide; ~1-centimeter apart) white laminae from the beginning of the zone at 29 to ~ 27.5 cal ka BP (see Appendix). During this period, percent carbonate values increased to ~22% and subsequently decreased to ~12%, and may reflect a transgressive-phase oscillation prior to the Stansbury oscillation (Fig. 9). MS values then decreased to ~0.8 SI at 27 cal ka BP, as percent carbonate values also decreased to ~14%. These fluctuations correspond to the widening of the laminae (~2-centimeters wide) beginning at 27.5 to 21.8 cal ka BP, and thus indicate a highly productive and deepening freshwater lake environment responding to increased winter precipitation (Patrickson et al., 2010). Increases in regional winter precipitation have been attributed to the changing size and shape of the Cordilleran and Laurentide ice sheets, which resulted in the repositioning of the jet stream's mean path over the Great Basin at ~28 cal ka BP (Nishizawa et al., 2013). Precipitation was further amplified by "lake effect storms", thus causing increases to lake size and glacial extent (Benson et al., 2011; Oviatt, 2007). Figure 15 demonstrates this increase in winter precipitation.

As the lake continued to transgress, all the water that infiltrated the system from direct precipitation, river runoff, and groundwater could exit only through evaporation (Oviatt, 2015). This hydrologically closed-basin made the lake vulnerable to changes in

the climate system, and thus, Lake Bonneville underwent a series of lake-level oscillations (Patrickson et al, 2010). The Stansbury oscillation is one of the best-dated oscillations of Lake Bonneville, consisting of at least two fluctuation events (Fig. 5) (Oviatt, 2015) that are present in the NRS14A zone II record. At 26 cal ka BP, lake levels are continuing to rise, evidenced by a decrease in percent carbonate values to ~14% (Fig. 9). However, lake levels begin to lower at 25 cal ka BP (the onset of the Stansbury oscillation), which is reflected in increasing percent carbonate values to 23%. MS values decreased to ~1.1 SI at this time to reflect low inputs of terrestrial sediment into the lake. Following this oscillation, percent carbonate values decrease to ~13%, and subsequently increased to ~21 at 23.5 cal ka BP to thus indicate the second fluctuation of the Stansbury oscillation event.

The Stansbury oscillation may correspond to the second oldest (H2) of six identified Heinrich events (Fig. 17; Patrickson et al., 2010). Heinrich events are recognized as global phenomena involving episodes of increased iceberg discharge, at periods of 5–10 k.y., in which large volumes of rock debris were deposited in North Atlantic sediments. Heinrich events occurred as the climate became progressively cooler (Bond and Lotti, 1995). Following these events, climate in the North Atlantic warmed abruptly to interglacial temperatures (Oviatt, 1997).

The mechanisms behind the Heinrich events are not fully understood, however, fluctuations in solar insolation, wind, and volcanic events have been proposed (Hemming, 2004). Other explanations suggest inputs of fresh water in the North Atlantic may have altered the ocean's heat conveyor, and thus resulted in abrupt changes in North Atlantic sea surface and air temperatures. The discharge from ice sheets, such as those in

Greenland or in Scandinavia, may have acted as a source for this freshwater, once these ice sheets collapsed every 2000 to 3000 years (Bond and Lotti, 1995). Evidence for dry climate conditions in the Great Basin have been linked to the initiation and termination of Heinrich events, (Oviatt, 1997; Zic et al., 2002), which may help to explain the Stansbury oscillation.

Additional Lake Bonneville oscillations have been correlated to abrupt reductions in ice-rafted debris in North Atlantic sediments (Oviatt, 1997). Oviatt (1997; 2015) identifies three falling-lake events, which are unnamed oscillations at approximately 22–22.5, 21.5, and 19 cal ka BP (U1, U2, and U3, respectively) (Fig. 12). The research of Oviatt (1997) suggests that these falling-lake events were synchronous with the termination of smaller-scale ice-rafting events, however, the ^{14}C dates provided by Oviatt postdate the Heinrich events (Benson et al., 2011). With the use of calibrated radiocarbon dates instead, it is possible to align the falling lake event (U3) with the beginning of a small-scale ice-rafting event, referred to by Bond and Lotti (1995), as lithic peak C. The other falling-lake events (U1 and U2) are associated with the termination of lithic cycle D, and the termination Heinrich event 2 (H2), respectively (Fig. 17; Bond and Lotti, 1995). Lithic cycle D occurred in the intervals between H2 and H3. The climate during the height of the Heinrich events and the smaller-scale events (C, D) became progressivity cooler, which may explain a rise in lake level prior to the oscillations. Abrupt warming occurred between Heinrich events, prior to lithic peak C, as well as warming at the termination of H2 and lithic peak D, and thus explains the brief lowering of lake levels during U1, U2, and U3 oscillations. Heinrich events are shown in Figure 17.

The unnamed oscillations (U1 and U2) can be identified in the NRS14A zone II record. The oscillation of U1 occurs at 22 cal ka BP, when percent carbonate values increase to ~20%, with no noticeable changes in MS values (Fig. 9). Likewise, the oscillation of U2 occurs at 21 cal ka BP, as percent carbonate values peak at ~19%. Conversely, the oscillation of U3 is not identifiable in the NRS14A zone II record, however, this oscillation may coincide with the Bonneville flood event at 18 cal ka BP. Furthermore, these oscillations are also apparent in the stratigraphy of the core as thin, coarse/sandy gray bands occurring at 21.4 cal ka BP and at 20.6 cal ka BP (see Appendix).

Following these transgressive-phase oscillations, Lake Bonneville further deepened and is characterized by greenish-gray clay beginning at 20.5 and leading up to 18.9 cal ka BP (see Appendix). Percent carbonate values remain low, at around ~14%, providing further evidence of deepening lake levels (Fig. 9). A slight increase in MS values to 23 SI occurs at ~19 cal ka BP and indicates rapid deposition of terrestrial sediment, or the deposition of volcanic ash from the Pahvant Butte volcanic eruption (Oviatt, 2015), which can be identified in the sediment core as a course/sandy gray band at 18.8 cal yr BP. The sediment then transitions to gray, sticky clay with carbonate rocks from 18.8–18.3 cal ka BP and corresponds to the highest point of the lake at ~18.4 cal ka BP, during which the Bonneville Shoreline formed. The catastrophic collapse of the natural dam near Red Rock Pass, Idaho and the resulting Bonneville flood took place at 18.6–17.1 cal ka BP (rounded to 18 cal ka BP), and is documented in the sediment core as a band of coarse/sandy, dark gray sediment (~1-centimeter wide) from 18.3–18.1 cal ka BP (see Appendix). After this flood event, percent carbonate values increase to ~20%,

indicating the lowering of lake levels to more saline conditions (Patrickson et al., 2010). Additionally, MS values decreased to ~5.5 SI at this time as a result of the flood removing sediment from the basin as water rushed into the Snake Drainage. Afterward, MS values then increased to ~62 SI (the highest MS value in the record) at 16.6 cal ka BP, and thus reflect the slump of sediment back into the basin after the flood event (Oviatt, 2015). The lake subsequently flowed out of the basin in the form of a river on landslide deposits for 3,000 years, resulting in reworked, gray clay beginning at 18.1 to 15.1 cal ka BP (see Appendix).

Fire episodes remained infrequent during NRS14A zone II, as evident by low charcoal values (Fig. 9). However, one fire episode is identified at 21 cal ka BP, with a peak magnitude of 0.2 particles^2/cm^2/episode (Fig. 10). This fire event may correspond to the abrupt warming associated with the termination of the H2 event at 21.5 cal yr BP. Charcoal influx, total influx pollen and the pollen ratios of Amaranthaceae to *Artemisia* are shown in Figure 16 to demonstrate the link between increased fire activity, greater amounts of vegetation, and a wet to dry climate. Accordingly, fires within the Bonneville basin during NRS14A zone II are most likely driven by wet climate conditions, which acted to provide enhanced growth of vegetation. A subsequent warm/dry climate period allowed for the ignition of the fuel, thus resulting in fire events. These climate oscillations are seemingly connected to the termination of H2 (Bond and Lotti, 1995; Oviatt, 1997).

Vegetation and Climate History

Climate during NRS14A zone II was cold and moderately wet, due to the increased regional winter precipitation caused by the southward shift of the jet stream's path over the Great Basin (Nishizawa et al., 2013). A conifer forest consisting of *Pinus, Picea,* and *Abies* (Fig. 14) expanded at or near the study site during this time, in the absence of shrub species (*Artemisia* and Amaranthaceae); however, Amaranthaceae briefly increased at ~19 cal ka BP during a warm period (Fig. 11). The absence of *Artemisia* and Amaranthaceae may be a result of these shrubs growing in the foothills, at higher elevations than present due to inundation of habitat from the lake. Overall, the pollen assemblage of NRS14A zone II is consistent with the few regional pollen records from this period, which indicate a shift from *Artemisia* to *Pinus* forest by ~30 cal ka BP (Beiswenger, 1991; Spencer et al., 1984; Thompson, 1990).

According to Minckley et al. (2008), the occurrence of high *Pinus* percentages suggests moderate-to-high annual precipitation and low-to-high July temperatures. Typically, high *Pinus* percentages occur in regions of moderate January precipitation to high July precipitation, which suggests that this pollen type is representative of annual precipitation, rather than seasonal precipitation (Minckley et al., 2008). The climate data obtained from NOAA National Climatic Data Center (2015) provides further detail into the climatic requirements of *Pinus* in Western North America. July temperatures for *Pinus* must be between 10–22 °Celsius and January temperatures between -15–5 °Celsius. Additionally, July precipitation for *Pinu*s is required to be in the range of 10–100 mm, while January precipitation is preferably 10–110 mm. Annual precipitation varies between 0–2000mm (Williams et al., 2006).

The pollen ratio of Amaranthaceae to *Artemisia* (Fig. 12) indicates a wet climate for most of the zone, with two distinct shifts of abrupt warming at 21.5 and 19 cal ka BP. These abrupt warming events correspond to the falling-lake events of U2 (21.5 cal ka BP) and U3 (19 cal ka BP), which were synchronous with the termination of the H2 event and the beginning of lithic peak C, respectively (Fig. 17; Bond and Lotti, 1995; Oviatt, 1997, 2015). As mentioned previously, the termination/initiation of Heinrich and smaller-scale ice-rafting events have been characterized by periods of aridity (Benson et al., 2011), with a return to a cooler climate, as evident in Figure 12.

This pattern of abrupt warming is also discernable in the pollen ratios of conifer to *Artemisia* + Amaranthaceae (Fig. 13), as well as the pollen ratio of Amaranthaceae to Poaceae (Fig. 15). These records indicate that the region experienced wet climate conditions, with increased winter precipitation, until 22 and 19 cal ka BP, when a shift towards abrupt warming occurred. The region briefly experienced dry climate conditions during this time that were marked by decreased winter precipitation (Fig. 15). Again, the abrupt warming corresponds to the pattern of falling-lake events of U1 (22–22.5 cal ka BP) and U3 (19 cal ka BP), that coincide with the terminations of lithic peak D and the beginning of lithic cycle C, respectively (Fig. 17; Bond and Lotti, 1995; Oviatt, 1997, 2015). It is also worth noting that the pattern of December insolation for 30°N increases concurrently with increases to the ratio of Poaceae pollen, therefore suggesting increased winter precipitation may be tied to increased December insolation (Fig. 15).

Overall, cooler and wetter climate conditions than present characterized NRS14A zone II, which facilitated the expansion of a conifer forest. However, brief warming episodes did occur and are associated with the beginning of the H2 event (~22.5 cal ka

BP), as well as smaller-scale ice-rafting events lithic peaks D (~21.5 cal ka BP) and C (~19 cal ka BP), which resulted in lake-level oscillations (Bond and Lotti, 1995, Oviatt, 1997, 2015). These warm episodes are most likely the result of a large percentage of the Laurentide Ice Sheet (LIS) losing mass to the North Atlantic during Heinrich events. The subsequent change in the size and shape of LIS may have increased evaporation rates as Lake Bonneville recovered from a Heinrich event, while also causing the jet stream to temporarily shift north of the Bonneville basin (Benson et al., 2011), acting to decrease winter precipitation (Fig. 15). In sum, wet events in the Bonneville basin have been linked with warm events in the North Atlantic (during the culmination of Heinrich events); and dry periods in the Bonneville basin have been linked with cold events in the North Atlantic (at the termination/beginning of Heinrich events) (Benson et al., 2011).

NRS14A Zone III: Early and Middle Holocene Xeric Shrub/Lake Bonneville-Wetland (Depth 221–49 cm, 16–6.0 cal ka BP)

Depositional and Disturbance History

Following the catastrophic flood event, lake levels dropped by over 130 m in less than a year (Oviatt, 2015). The Provo shoreline developed at 15 cal ka BP in the basin, as the lake transitioned to the regressive phase (Godsey et al, 2011). Lake sediments from this time at NRS14A zone III are composed of gray clay that shifted to light greenish-gray clay from 15.1 to 13.4 cal ka BP (see Appendix). Percent carbonate values increased to ~23% at 15 cal ka, with a spike to 25% at 14.5 cal ka BP, while MS values also increased to 21 SI to indicate the stabilization of lower lake levels at the Provo Shoreline (Fig. 9). The development of the Provo Shoreline may be associated with the termination of a smaller-scale Heinrich event, known as lithic peak A, which occurred ~15.5 cal ka

BP (Fig. 17; Bond and Lotti, 1995).

Lake Bonneville then regressed to altitudes of 1280 masl, comparable to those of the modern Great Salt Lake by 13 cal ka BP (Oviatt, 2015). Four distinct sandy, dark gray bands occur: 13.9, 13.8, 13.7, and 13. 75 cal ka BP to further support the existence of a rapidly regressing lake at this time.

Once Lake Bonneville fell below the topographic threshold between the Sevier and GSL basins during the Younger Dryas (12.9–11.6 cal ka BP), resulting in two sub-basin fresh water lakes: an overflowing lake in the Sevier basin (Lake Gunnison) and a rapidly regressing lake in the Great Salt Lake basin (Lake Gilbert) (Goebel et al., 2011). Lake Gilbert (located north of NRS14A; Fig. 3) transgressed to approximately 1300 masl and subsequently stabilized at the Gilbert shoreline. The transgression event of Lake Gilbert may be connected to an abrupt return to glacial conditions during the Younger Dryas (Oviatt et al. 2005). During this same time, Lake Gunnison (located southwest of NRS14A; Fig. 3) overflowed to the north at the Old River Bed Threshold. These dramatic changes are documented in the stratigraphy of the sediment core at 13.4 –12.6 cal ka BP, when the sediment swiftly transitioned to extremely gritty/gray deposits, interspersed with carbonate rocks (see Appendix). A decrease in percent carbonate values to 13%, and an increase in MS to ~26 occurred at ~13 cal ka BP, reflecting the rapid drop in lake levels as Lake Bonneville split into two smaller, freshwater lakes.

The North Redden Springs study site experienced additional hydrological changes once Lake Bonneville evaporated. The stratigraphy of the sediment core transitioned to pale green clay/marl at 12. 6 to 7.4 cal ka BP. A coarse dark gray band is present at 12.2–12 cal ka BP, and a gray band at 7.4–7.3 cal ka BP. Percent carbonate values fluctuated

between ~15%–10%, while MS values fluctuated between ~10–4 SI (Fig. 9), reflecting the formation of either a fairly deep lake, marsh, or wet meadow at the study site by ~12 cal ka BP. A large volume of ground water previously stored in piedmont and mountain aquifers was discharged onto the basin floor during this period to facilitate the formation of the various lake/marsh/meadow environments (Reheis et al., 2014). Once the Younger Dryas ended ~11.0–10.2 cal ka BP, notable changes occurred in the Bonneville basin and include the retreat of Lake Gunnison and the formation of the Great Salt Lake when Lake Gilbert fell below 1287 masl (Goebel et al., 2011). Additionally, from ~9.5 to 8.5 cal ka BP, large wetland systems throughout the Great Basin, such as the Old River Bed Delta, contracted or dried up (Oviatt et al., 2003; Rhode et al.,2005; Thompson, 1992; Wigand and Rhode, 2002).

The end of NRS14A zone III is marked by a depositional hiatus at ~5.8 to 7.1 cal ka BP. The stratigraphy of the core consisted of loamy/chalky greenish-gray marl from 7.3 to 5.8 cal ka BP. Percent carbonate values range from 10–13%, while MS values (7 SI) and percent organics (4%) remain at a constant rate to reflect a water-saturated area of low productivity. This dry period is consistent with regional dry events (Beiswenger, 1991; Louderback and Rhode, 2009; Madsen and Currey, 1979; Thompson, 1990).

Fire activity increased in NRS14A zone III. Charcoal values increased at 13.8 ka to 0.3 particle/cm^2/yr, at 11.8 ka (0.5 particle/cm^2/yr) and at 7.5 ka (0.7 particle/cm^2/yr) (Fig. 9). Fire episodes were identified at 15, 12, 11.5, 10, 7.5, and 6 cal ka BP (Fig. 10). Peak magnitudes varied from 0 to 20.0 (particles/cm^2/episode).

The fire episode at 15 cal ka BP may be associated with the termination of a small scale Heinrich event (~15.5 cal ka BP), known as lithic peak A (Bond and Lotti, 1995).

This period was marked by a clear warming event, based on the ratio of more Amaranthaceae to *Artemisia* pollen (Fig. 12).

Fire episodes at 12, 11.5, 10, 7.5, and 6 cal ka BP (Fig. 11) all occurred during dry periods in the Bonneville basin, with most fire events occurring in parallel to increases in vegetation (Fig. 16). The possible mechanisms driving fire frequency could have included increases in xeric-shrub fuels (Amaranthaceae), as well as dry conditions. Dry fuels require less energy input to reach ignition temperature. Additionally, wetland ecosystems in the Bonneville basin sustained significant numbers of Paleoindian people as early as 12 to 11 cal ka BP (Oviatt et al., 2003), and anthropogenic burning may play a role in the increasing fire episodes of NRS14A zone III. Also of importance is the observation that fire episodes occurred before and after the depositional hiatus of the spring (~5.8–7.1 cal ka BP) (Fig. 10). This may indicate increasing aridity, or the lack of viable fuel sources during the hiatus.

Vegetation and Climate History

During NRS14A zone III, the climate transitioned from cold and wet glacial conditions to warmer and drier interglacial conditions. A substantial decrease in *Pinus*, *Abies,* and *Picea* forests is documented, while lowland soils were exposed and became more alkaline, thus allowing the growth of halophytic shrub communities (Amaranthaceae) at ~16 cal ka BP (Fig. 11). Additionally, *Populus* (cottonwood) appeared in the record and was most likely growing in gallery forests in close proximity to the newly formed springs within the basin. At 14 cal ka BP, xeric woodland species of Cupressaceae and *Quercus,* as well as dryland shrub, herb and grass taxa (Rosaceae,

Sarcobatus, Asteraceae, and Poaceae) increased. The presence of *Botryococcus*, Cyperaceae, and Typhaceae signal the presence of a shallow lake/marsh environment as early as 16 cal ka BP at the study site. A further insight includes the establishment of Apiaceae cf *P. bolanderi* (Yampah) at 16 cal ka BP, likely an important food source for Paleo-Indians.

The lowering and eventual evaporation of Lake Bonneville contributed to an alkaline, lowland environment that supported the establishment of xeric shrub communities dominated by Amaranthaceae at North Redden Springs. Minckley et al. (2008) suggest that Amaranthaceae pollen is indicative of open, arid vegetation types and desert environments of limited moisture. The specific climate conditions to which Amaranthaceae is most suited include July temperatures between 18–32 °Celsius and January temperatures between -15–10 °Celsius. July Precipitation must be between 30–100 mm, with January precipitation in the range of 4–30 mm. Lastly, Amaranthaceae require annual precipitation to be 1000 mm (Williams et al., 2006).

Based upon the pollen ratio of Amaranthaceae to *Artemisia,* a rapid shift towards drier conditions occurred at 15 cal ka BP, and may have been connected with the termination of a small scale Heinrich event (lithic peak A) (Fig. 12; Fig. 17). This event contributed to a pattern of abrupt warming in the Bonneville basin at this time (Zic et al., 2002; Oviatt, 1997; Bond and Lotti, 1995). The climate subsequently shifted to wetter conditions (more *Artemisia* pollen) at 14.5 cal ka BP, once Heinrich event 1 (H1) reached its highest point (Fig. 17; Bond and Lotti, 1995). Drier conditions returned at 14 cal ka BP, as the pollen ratios shifted towards more Amaranthaceae pollen (Fig. 12). However, at ~10 cal ka BP the ratio shifted towards more *Artemisia* pollen, but does not exceed the

zonal average. This may represent early Holocene wet climate conditions. These climate patterns are mirrored in the pollen ratio of conifers to *Artemisia* + Amaranthaceae (Fig. 13), with dry conditions present at 15 cal ka BP, wet conditions at 14.5 cal ka BP and subsequent dry conditions after 14.5 BP.

Comparable climate trends are apparent in the pollen ratio of Cupressaceae to *Pinus* (Fig. 14), however, this ratio is more sensitive to changes in effective moisture. The ratio documents an abrupt dry period at ~14 cal ka BP, which was followed by an abrupt wet period at ~13.7 cal ka BP. A subsequent rapid warm period occurred at 13.5 cal ka BP, and coincides with the termination of H1 (Fig. 17; Bond and Lotti, 1995). A shift toward wetter conditions transpired by ~13 cal ka BP. Warmer and drier conditions are evident from 12–6 cal ka BP, as the climate began the interglacial Holocene period.

In addition, the pollen ratio of Amaranthaceae to Poaceae (Fig. 15) demonstrated drying at 15 cal ka BP (less winter precipitation), followed by wetter conditions (more winter precipitation) at 14.5 cal yr BP, with a brief period of dry to wet conditions (~14 and ~13.7, respectively). Winter precipitation increased from ~13.5–12.5, however, a subsequent transition to less winter precipitation occurred from 12.5 to 6 cal ka BP. Overall, these climate fluctuations follow approximately the same patterns as the previously discussed pollen ratios, however, some differences may be attributed to different vegetation types responding more rapidly and (or) slowly to changes in effective moisture. Furthermore, December insolation for 30° N began to decrease at 16 cal ka BP and reached a low point of ~207 W/m² at ~11 cal ka BP, when more Amaranthaceae pollen was abundant in the record (Fig. 15). This suggests that decreased December insolation and increased summer precipitation is important for the growth of these xeric

shrubs.

The pollen record from NRS14A zone III follows many of the same trends as the regional records, however, differences in elevation, terrain and precipitation may have contributed to the early establishment of a xeric shrubland at the North Redden study site. The regional pollen records within the Bonneville basin and nearby vicinity suggest a trend of abundant sagebrush and conifer pollen before ~13 cal ka BP, with a subsequent increase in xeric shrubs to present (Beiswenger, 1991; Bright, 1966; Madsen and Currey, 1979; Spencer et al., 1984; Thompson, 1992). For instance, the 15,000-year pollen record by Louderback and Rhode (2009) indicated that the Blue Lake marsh system in the Western Great Salt Lake desert became dominated by terrestrial plant communities of pine and sagebrush during the latest Pleistocene, and later transitioned to wetland plant communities, with increases in shadscale and other dryland shrubs beginning at ~11.9 cal ka BP to present. Additionally, the Great Salt Lake Core C from Spencer et al. (1984) shows a decline in conifer woodlands as xerophytic shrubs expanded in the Bonneville basin after 11 cal ka BP. The pollen record from Swan Lake (Bright, 1966) also demonstrates a decrease in pine as sagebrush and grass increase at ~12.1 cal ka. The Swan Lake record similarly shows a subsequent increase in Amaranthaceae pollen from saltbrush, as well as an increase in Poaceae pollen from grass when lowland soils became more alkaline. Furthermore, the pollen record from Grays Lake in southeastern Idaho (Beiswenger, 1991) suggests warming at ~9.5 cal ka BP, as sagebrush steppe shifted to sagebrush/shadscale steppe. Lastly, the pollen record of Madsen and Currey (1979) indicates that after 8.8 cal ka BP the ratio of conifer pollen to all other pollen showed a swift transition from early Holocene cool temperatures to extreme warm temperatures at

Snowbird Bog in the Wasatch Range, Utah. In sum, the climate of the Early Holocene was cooler than today, and possibly wetter, fostering more diversified vegetation types, and a dominance of Rocky Mountain juniper. By ~8.5 ka, the pollen records establish a region-wide pattern toward warmer temperatures, with less effective moisture throughout the Middle Holocene (Rhode, 2000b).

Moreover, many of the plant-based studies for the Bonneville basin have focused on the early Holocene (10,000–8,000 yr BP) rapid shift from glacial to interglacial climates (Rhode, 2000b). Antevs (1955) proposed that the climate of the early Holocene was cooler and wetter than modern, transitioning between the glacial late Wisconsin and the warmer drier middle Holocene. Subsequent work is largely in agreement with a cool, wet early Holocene (e.g., Rhode, 2000), which is evident in the North Redden record as an increase in *Abie*s pollen percentages from 10 to 8 cal ka BP (Fig. 12). Data from packrat midden records indicate that this cool, moist climate encouraged the growth of conifers, such as limber pine and bristlecone pine at lower elevations than those taxa are found in modern habitats (Rhode, 2000b). Additionally, the upland vegetation of the Bonneville basin consisted of mesophilic shrubs, stands of aspen and mountain mahogany, as well as Rocky Mountain juniper and Utah juniper. Lowland areas were dominated by sagebrush steppe, grasses and saltbush scrub communities. Greasewood and other halophytic vegetation (Amaranthaceae) dominated large expanses of playa margin around the dry lake bed of Lake Gilbert at ~10 cal ka BP (Fig. 3). In addition, the cooler, wetter climate supported extensive wetlands in certain valleys, such as the Dugway Proving Ground (DPG) wetlands (Fig. 3), which likely had a higher water table (Rhode, 2000b).

In summary, the climate of NRS14A zone III can be described as transitional between wet and cold glacial to warmer and drier interglacial conditions. The increased pollen percentages of Amaranthaceae suggest an arid lowland environment of alkaline soils. Additionally, the presence of aquatics, and the appearance of more diversified vegetation types indicate a shallow lake/wetland system as early as 16 cal ka BP. Complex climate forcing mechanisms characterized NRS14A zone III, including warming associated with the termination of the small scale Heinrich event (lithic peak A) at 15 cal ka BP, a wet period at 14.5 cal ka BP during the high point of (H1), an abrupt warm period associated the termination of H1 at 13.5 cal ka BP, and dry/warm conditions after 12 cal ka BP. A general trend toward increased warming and drying supported increased fire activity and the establishment of xeric shrubs during NRS14A zone III.

Paleo-Indians

Paleo-Indians began arriving in the West Desert, Utah as early as 12 to 11 cal ka BP (Oviatt et al., 2003), when the climate was transitioning from glacial to interglacial conditions. Shallow lakes, marshes and (or) wet meadow environments began forming once groundwater was released onto the basin floor and Lake Bonneville evaporated. Accordingly, the NRS14A study site was a suitable environment for the habitation of Paleo-Indian populations. As early as 16 cal ka BP, the study site consisted of aquatic vegetation growing in a shallow lake/marsh/wet meadow environment, with surrounding vegetation consisting of xeric shrub communities of Amaranthaceae. Gallery forests of *Populus* (cottonwood) grew in close proximity to the study site, near the newly formed springs of the area. Additionally, pollen of Apiaceae cf *P. bolanderi* (Yampah) appears in the record at 16 cal ka BP and may represent early appearance of this important food

source for Paleo-Indians in this region.

With the arrival of Paleo-Indians in the Bonneville basin, a coincident increase in fire episodes occurred, specifically at 12, 11.5, 10, 7.5, and 6 cal ka BP (Fig. 10). Anthropogenic burning may have been responsible for this increase in fire frequency.

It also may be worth noting that at the time of the depositional hiatus at NRS14A from ~5.8 to 7.1 cal ka BP, archaeological records indicate a parallel decrease in human occupation of the NRS14A study site (J. DeGraffenried, personal communication, May 8, 2015).

NRS14A Zone IV: Late Holocene Xeric Shrub/Wetland-Spring

(Depth 49–0 cm, 6.0 cal ka BP–Present)

Depositional and Disturbance History

NRS14A zone IV begins at the termination of the wetland hiatus and consists of greenish gray, loamy marl from 5.8–2.7 cal ka BP (see Appendix). Percent carbonate values were moderate at ~14% at 6 cal ka BP, however, values decreased to 3% by 3.5 cal ka BP (Fig. 9) to suggest increased water depths of the wetland, based upon previous research which has indicated that carbonate values are inversely correlated with changes in lake level (Oviatt, 1997). Additionally, cooler climate conditions and greater effective moisture after 5.5 cal ka BP have been documented (Rhode, 2000b) and may explain increasing water depths at this time. Throughout this period, percent organics and MS values remained at 4% and 8 SI, respectively. From 2.7 cal ka BP to AD 1989, the sediment transitioned to dark gray/brown loamy clay, with areas of sand/silt to signal the activation of the spring. As the sediment transitioned to wetland/spring deposits, MS, and percent carbonate values remained constant, however percent organic values decreased

slightly to ~2% beginning at 2.0 cal ka BP to 1.0 cal ka BP (AD 950).

The spring became shallow and saline at 1.0 cal ka BP (AD 950), as the sediment eventually shifted to brownish/black deposits (from AD 1985 to present), with a dense root mat (from AD 1995 to present). An increase in percent carbonate values to < 15% occurred at 1.0 cal ka BP to 150 cal BP (AD 950 to 1800). Similarly, percent organics increased to ~6%, and MS values increased to 30 SI at 1.0 cal ka BP (Fig. 9). The changes in these proxies indicate a moderately productive, shallow, and saline spring, in which greater amounts of terrestrial sediment was accumulating due to upland erosion.

During the historical period, the spring deepened and increased in productivity, as evident by a decrease in percent carbonate to >3%, while percent organics increase substantially to < 20% (Fig. 9). MS values decreased from 30 SI to 7–13 SI. Therefore, it can be concluded that a deeper and highly active freshwater spring, with less input from terrestrial sources (erosion), was established by 150 calibrated radiocarbon years before present cal BP (~AD 1800 to present).

Once the NRS14A spring activated, fires became frequent during NRS14A zone IV. This is evidenced by increased charcoal values beginning at 4 cal ka BP and lasting to present (Figs. 9, 10). A notable increase in both charcoal accumulation rates and MS values occurred at 150 cal BP (AD 1800), which suggests erosional events occurred in response to fire activity at this time (Fig. 10). Additionally, a significant increase in charcoal accumulation is observed in the modern samples, with peak magnitudes over 40 (particles/cm^2/episode). Three fire episodes were identified in the record at 6, 3.8 and 2.5 cal ka BP, with peak magnitudes of 0.5, 0.0, and 0.2 (particles/cm^2/episode), respectively (Fig. 10). These fire events may be attributed to wet-dry climate conditions, combined

with greater amounts of available fuel (xeric shrubs, low-lying herbs and grasses) on the landscape (Fig. 16). Of the limited fire history studies within the eastern Great Basin, the fire reconstruction of a sagebrush-dominated valley in central Nevada by Mensing (2006) indicated similar findings. Results from his 5,500-year study suggest that the fire regime in central Nevada is climate-and fuel-driven, with an increase in sagebrush and fire during wetter climate periods and a decrease in sagebrush and fires during extensive dry periods. Additionally, the charcoal record from Mensing (2006) indicates that fires have increased in frequency within the historic period. However, in comparison to this 5,500-year study of fire occurring in sagebrush-dominated vegetation communities, the North Redden fire history reconstruction has been completed for a spring dominated by halophytic playa-margin plants during the last 36,800 years.

Other mechanisms impacting the fire regime during NRS14A zone IV could have included anthropogenic burning. Late prehistoric hunter/gatherers were established in the Bonneville basin after 2.0 cal ka BP (Louderback and Rhode, 2009; Louderback et al., 2010), and may have begun altering the landscape through the use of fire. Likewise, increased fire activity in the historical samples can be attributed to European settlement within the basin. Additionally, the introduction of invasive species, such as cheat grass, as well as historic fire suppression likely contributed to changes in the fire regime in such a way to cause frequent and higher intensity fires.

Vegetation and Climate History

Arid climate conditions with less effective moisture defined NRS14A zone IV, as evident by a xeric shrubland of Amaranthaceae (e.g., shadscale, saltbrush) and

Sarcobataceae (e.g., greasewood). However, wet and cool periods occurred at 6.0–2.0 cal ka BP, which corresponds to the "Neoglacial" advances that occurred at 3300–2400 radiocarbon years before present (ka BP) and at 3600–2800 ka BP (Currey and James, 1982; Fowler, 1977). These wetter-than-present periods have been attributed to increases in summer moisture (Rhode, 2000b), and may explain the activation of the NRS14A spring at ~2.0 cal ka BP.

In response to the warmer and drier conditions of the mid to late Holocene, the pollen percentages of xeric shrubs (Amaranthaceae) increased significantly during NRS14A zone IV (Fig. 11). Additionally, arboreal pollen percentages (*Pinus*, *Abies*, *Picea,* and *Populus*) increased from the previous zone, as a possible response to the wet conditions. Invasive species, such as Elaegnaceae cf *Elaeagnus angustifolia* (russian olive) first appear in the record at ~AD 1641 (309 cal BP) and became established in the area by ~AD 1990 (-40 cal ka BP), which is consistent with the introduction of the invasive tree species in Utah in the late 1800s (Nagler et al. 2011). After 1.0 cal ka BP (AD 950), pollen percentages for trees, shrubs, herbs and aquatics increased concurrently and included Cupressaceae, *Quercus*, *Ambrosia*, Roseaceae, *Sarcobatus*, Asteraceae, Poaceae, *Botryococcus*, and Cyperaceae. These increases correspond to the activation and amplified productivity of the NRS14A spring, as well as wet climate conditions after 1.0 cal ka BP. Furthermore, Apiaceae cf *P. bolanderi* (Yampah) re-appears in the record from 7.4 to 900 cal ka BP (AD 1050) and may have been used as a food source for Paleo-Indian, Archaic and late prehistoric hunter/gatherer populations.

The warmer and drier climate conditions can be observed in the pollen ratio of Amaranthaceae to *Artemisia*, with a large influx of Amaranthaceae pollen throughout

NRS14A zone IV (Fig. 12). By ~1.0 cal ka BP (AD 950), conditions became increasingly arid, which coincides with the period of increased erosional and fire activity, as well as a shallow, saline spring during this time. Conditions shifted towards slightly less arid at ~150 cal BP (AD 1800) to present, the same time in which the productivity and water depth of the NRS14A spring increased. This may coincide with a cool period during the Little Ice Age (600–100 cal BP) (Rhode, 2000b). Likewise, the pollen ratios of conifer to *Artemisia* + Amaranthaceae document increased aridity at ~1.0 cal ka BP (Fig. 13).

The regional terrestrial pollen records of the Bonneville basin have documented similar climatic fluctuations that included warmer and drier climate conditions during the middle Holocene (8.0–4.0 cal ka BP), in which environments in the Great Basin experienced an expansion of xeric-adapted vegetation. Lowlands were dominated by Amaranthaceae shrubs, as sagebrush and grass decreased, while upland communities consisted of juniper woodlands and shrubs (Rhode, 2000b). However, pollen records from the eastern Great Basin are not uniform in this drying pattern. The Blue Lake record shows a climate amelioration, or periods of greater moisture at 6.5 cal ka BP, as sagebrush increased (Louderback and Rhode, 2009). In a similar fashion, the pollen record from the Great Salt Lake (Mehringer, 1985) indicated an increase in pollen abundance, which also suggests cooler and wetter conditions after ~5.7 cal ka BP. The record from Snowbird Bog suggests a warm and dry period from ~8.8 to 6.8 cal ka BP, while the period up to 6.0 cal ka BP was cooler and wetter (Madsen and Currey, 1979). Conversely, the pollen record from Bright (1966) suggests that, between 7.8 and 3.1 ka, grass was replaced with more alkali-loving plants, as alkalinity increased (Rhode, 2000b). Additionally, the sediments from Ruby Marsh in northeast Nevada indicate low water

levels with an expanse of shadscale beginning at ~7.8 cal ka BP and lasting to ~4.6 cal ka BP (Thompson, 1992). Similar climate ameliorations can be detected in the NRS14A zone IV ratio of Cupressaceae to *Pinus* pollen (Fig. 15).

The anomalously mesic interval that occurred from ~6 to 5.5ka suggests that after 5.5ka, the climate became cooler, with greater effective moisture than the early part of the Middle Holocene. Rhode (2000b) has described this as a Late Holocene cool-wet episode. This cooler and wetter period than previous can be identified in the NRS14A zone IV pollen ratio of Cupressaceae to *Pinu*s, when the ratios shift towards more *Pinus* pollen at the beginning of the zone ~6.0 to 2.0 cal ka BP (Fig. 14). Within this time period, the NRS14A wetland increased in water depth at ~3.5–1.5 cal ka BP. An analogous mesic interval has been recorded in the regional pollen records, such as increasing water depth and expansion of sagebrush at Ruby Marsh at 4.6 cal ka BP (Thompson, 1992). Additionally, the Blue Lake record shows environmental fluctuations with cool periods from ~4.4 to 3.4 and ~2.7 to 1.5 cal ka BP, with warmer conditions from 3.4 to 2.7 and after 1.5 cal ka BP (Louderback and Rhode, 2009). Similarly, the late Holocene records from the Great Salt Lake and Crescent Springs (Mehringer, 1985) indicate an increase in sagebrush and conifers, with declining *Amaranthus* at ~4.4 cal ka BP. Subsequent fluctuations indicate cool/wet conditions at ~3.9, ~2.8, ~2.2, and ~1.4 cal ka BP, with warm periods occurring at ~3.4, ~2.6, and ~1.8 cal ka BP. At Swan Lake (Bright, 1966), conditions became cool by 3.1 cal ka BP as grasses increased and shadscale scrub and sagebrush steppe decreased. Following these cool-wet episodes, the Bonneville basin returned to warm and dry conditions at 1.7 cal ka BP, when shrub steppe vegetation increased and limber pine decreased (Rhode, 2000b).

In contrast to this documented cool-wet period, additional studies of the Great Basin have indicated century-scale periods of drought at 3.5 cal ka BP (Benson et al., 2002; Tausch et al., 2004), and from 2.5 to 1.8 cal ka BP (Mensing et al., 2008; Tausch et al., 2004), and at ~1.2 cal ka BP (Louderback and Rhode, 2009). These studies suggest that periods of drought in the western Great Basin did not necessarily impact the eastern Great Basin in similar ways. The pattern of late Holocene environmental change across the eastern Great Basin was likely spatially and temporally heterogeneous.

The NRS14A zone IV record aligns with the climate patterns observed in the eastern Great Basin pollen records, which indicate a cool-wet episode was followed by warmer conditions (Bright, 1966; Louderback and Rhode, 2009; Mehringer, 1985; Thompson, 1992). The pollen ratios of Cupressaceae to *Pinus* pollen depict fairly abrupt warmer and drier than previous climate conditions at ~1.0 cal ka BP (Fig. 14). This warming coincides with decreases in all pollen types except Amaranthaceae (Fig. 11). The site then transitioned to wet conditions once more at ~150 cal BP (AD 1800) to present, when many pollen types began increasing, thus suggesting a return to a wetter climate (Fig. 11). December insolation for 30 °N began increasing at 6.0 cal ka BP and reached a high of 225 W/m² at ~150 cal BP (Fig. 15). This increase in insolation, along with cool/wet climate conditions, resulted in an expansion of Poaceae in the modern samples. Increased pollen percentages of Poaceae may also be a result of the more frequent fire regimes present at this time, as pyrophilic grasses responded to increased fire activity (Fig. 11).

In sum, climate during NRS14A zone IV can be described as warmer and drier than the previous zone, with periods that were wetter than present at the beginning at ~

6.0 cal ka BP to 2.0 cal ka BP. The wetland deepened from ~3.5–1.5 cal ka BP, as a response to increased summer moisture (Rhode, 2000b). At ~2.0 cal ka BP, the spring activated, and consisted of standing freshwater. However, the spring became shallow from ~1000–150 cal BP (AD ~950–1800) due to a period of increased aridity. A wet period occurred at ~150 cal BP (AD 1800) and spring productivity and water depth has increased to present. Fires began increasing in frequency at ~4.0 cal ka BP to present, as a response to the drier climate interspersed with wet periods, as well as the presence of viable fuel sources and (or) anthropogenic burning. Overall pollen percentages increased during NRS14A zone IV, with dominant vegetation consisting of xeric shrubs (Amaranthaceae) and aquatics. These vegetation and climate patterns correspond to the regional records that describe the middle Holocene as warmer and drier than today, while the late Holocene experienced a cool-wet episode. The vegetation in the Bonneville basin reached its more or less modern distribution with certain notable exceptions; Mormon tea, Utah juniper, and Rocky Mountain Juniper had not yet reached their modern range (Rhode, 2000b). The latest Holocene (2.0 yr BP–Present) has been characterized by warmer and drier conditions than the late Holocene. Climate at this time has not been stable, with less effective moisture occurring during the past 2000 years and a cool period during the Little Ice Age, from 600–100 cal BP (Rhode, 2000). Vegetation communities reached their modern distributions by 2000 years ago, and, within the last 150 years non-native plants may have contributed to the greatest changes in Bonneville basin vegetation since the Pleistocene/Holocene transition (Rhode, 2000b).

Late Prehistoric Hunter/Gatherers

Fremont hunter/gathers were present in the Bonneville basin after 2.0 cal ka BP, which coincided with the activation of the freshwater NRS14A spring. Additionally, 2.0 cal ka BP was a relatively wet period and thus made the Bonneville basin a hospitable place to live. During the period of aridity around ~1.0 cal BP, the spring became shallow and saline and thus may have been unsuitable for habitation. Once the spring returned to deeper-water conditions during the wet period by ~150 cal BP, hospitable conditions most likely resumed. Apiaceae cf *P. bolanderi* (Yampah) appears in the record from 7400–900 cal BP and might have been used as a food source for Paleo-Indian and Fremont populations. However, the lack of Apiaceae after 900 cal BP may indicate unsuitable environmental conditions, due to the period of increased aridity, which corresponds to the decline in human populations and a retreat of regional marsh systems after 9ka (Louderback et al., 2010).

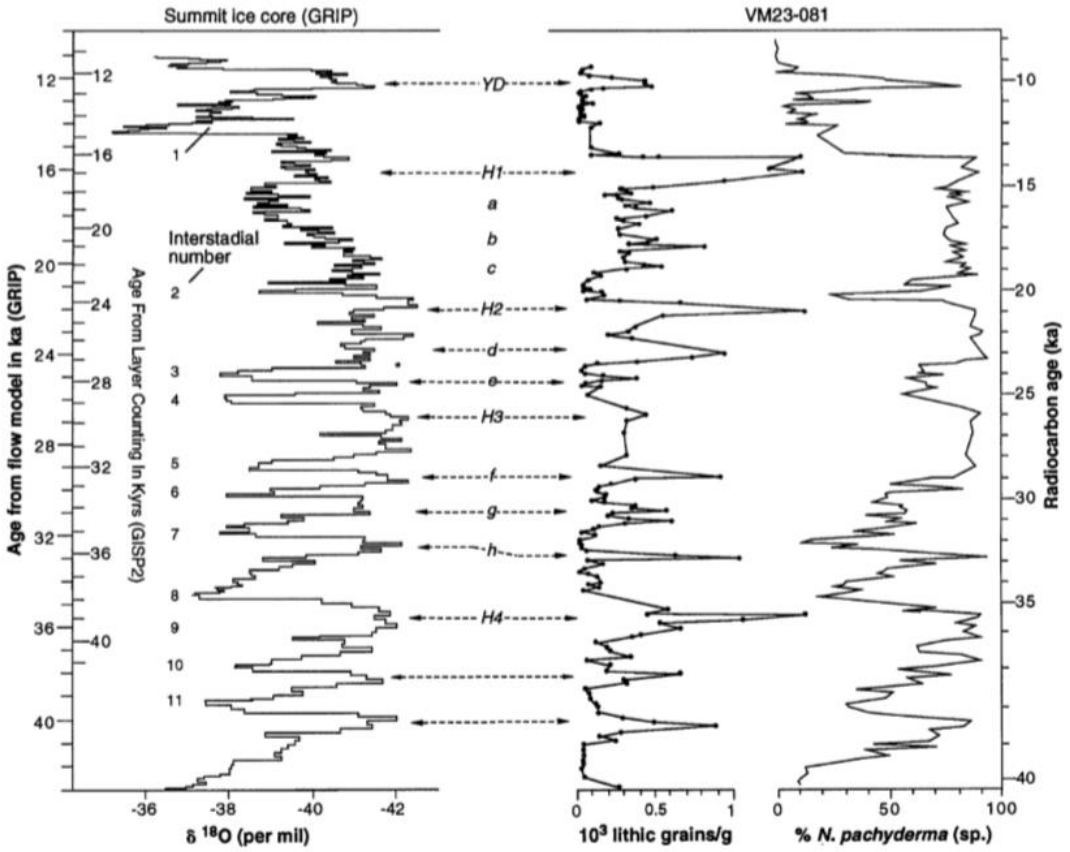

Figure 17. Comparison of the oxygen isotope record and age model for the GRIP ice core, Summit, Greenland, with measurements of lithic concentrations and percentages of planktonic foraminifera. Cycles between Heinrich events are given letters to aid their description (Bond and Lotti, 1995).

CONCLUSIONS

This study described the chronology of Pleistocene Lake Bonneville and the Holocene wetland of North Redden Springs, within the Bonneville basin, as well as the environmental changes associated with fire, vegetation, and climate from a 36,800-year record. Objective one of this study has been satisfied through the analyses of pollen, macroscopic charcoal, magnetic susceptibility, and loss-on-ignition. The results of these reconstructions have provided an in-depth description of the paleoenvironmental history of the North Redden Springs region to further understand past gradual and abrupt climatic, hydrologic, and biotic changes occurring within the Bonneville basin. Objective two has been satisfied through (1) processing 23 AMS radiocarbon dates, which provided chronological control for the sediments, and (2) through the assessment of the paleoenvironmental data to therefore refine the chronology of Lake Bonneville. Lastly, objective 3 was completed through the evaluation of the paleoenvironmental data to provide further insights into spring activity, and environmental conditions of North Redden Springs, and how these changes may have impacted prehistoric human populations within the region. The North Redden core has extended the record of fire and vegetation change for the Bonneville basin to ~36.8 cal ka BP, and thus represents one of the few environmental records in the Bonneville basin to examine fire and vegetation change on such a long-term scale.

In summary, during the late Pleistocene (36,813–29,000 cal yr BP), a cold-

adapted sagebrush steppe surrounded a shallow lake at the study site. The lake transgressed at 34.5 cal ka BP, however lake levels lowered at 32.5 cal ka BP. Lake levels began rising rapidly at ~31 cal ka BP, due to increased spring/summer precipitation from the tropical eastern Pacific and the Gulf of Mexico, which dominated the Bonneville basin between ~50–28 cal ka BP (Nishizawa et al. 2013). The formation of a pluvial lake within the Bonneville basin began sometime prior to 36.8 cal ka BP.

A subsequent increase in winter precipitation from the southward shift of the jet stream during the latest Pleistocene (29,000–16,000 cal yr BP), as well as the diversion of the upper Bear River during the Hansel Valley volcanic eruption, resulted in the expansion of conifer forest and deeper lake levels. Lake Bonneville experienced a series of lake-level fluctuations, including the Stansbury oscillation (25 cal ka BP), U1 (22–22.5 cal ka BP), U2 (21.5 cal ka BP), U3 (19 cal ka BP), high stand at Bonneville Shoreline (18.4 cal ka B), and the Bonneville flood (18 cal ka BP). Abrupt warming episodes associated with North Atlantic ice-rafting events occurred in parallel to many of these lake-level changes and include the beginning of the H2 event (~25 cal ka BP), the termination of lithic cycle D (~22–22.5 cal ka BP), the termination of H2 (~21.5 cal ka BP), and lithic peak C (~19 cal ka BP). One fire episode occurred at 21 cal ka BP and is associated with a wet period followed by abrupt warming.

During the middle and early Holocene (16,000–6,000 cal yr BP), the climate was transitional between glacial wet and cold to interglacial warm and dry climates. As early as 16 cal ka BP, a xeric shrub steppe composed of halophytic Amaranthaceae (e.g., shadscale, saltbrush) and Sarcobataceae (e.g., greasewood) vegetation dominated large expanses of playa around the North Redden lake-wetland complex. Lake Bonneville

experienced additional dramatic changes in lake levels, including the formation of the Provo Shoreline (15 cal ka BP), the division into Lake Gunnison and Lake Gilbert (~12.9–11.6 cal ka BP), and the formation of the Great Salt Lake (~11.0–10.2 cal ka BP). These changes in lake levels, as well as changes in the vegetation regime and deposition of the North Redden wetland coincided with variations in the climate system, including warming linked with the termination of lithic peak A (~15 cal ka BP), a wet period associated with H1 (14.5 cal ka BP), an abrupt warm period associated the termination of H1 (13.5 cal ka BP), and warmer/drier conditions after 12 cal ka BP. Fire activity intensified as the landscape transitioned from a forested community to a xeric shrub/grassland.

The late Holocene (6000 cal BP–present) was characterized as a period of increased aridity, interspersed with cool-wet episodes. A xeric shrub steppe (Amaranthaceae) expanded its range to become the dominant vegetation type on the landscape. Substantial increases in aquatics and other diversified vegetation types also occurred in response to increases in summer moisture, which also caused the North Redden wetland to deepened from ~3.5–1.5 cal ka BP. The spring activated at ~2.0 cal ka BP, during the cool-wet episode. A period of aridity was documented at ~1000–150 cal ka BP (AD 950–1800), and is responsible for the shallow and saline conditions of the spring. Spring productivity and water depth increased once more during a cool-wet episode at ~150 cal BP. Fires continued to increase in frequency and intensity throughout the historical period. Mechanisms behind fire activity likely included wet climate episodes, which acted to provide ample fuel sources, while subsequent dry climate episodes provided ignition sources. Additionally, anthropogenic burning, fire

suppression, and invasive plant species may have contributed to the increased fire activity.

APPENDIX

STRATIGRAPHY OF NRS14A CORE

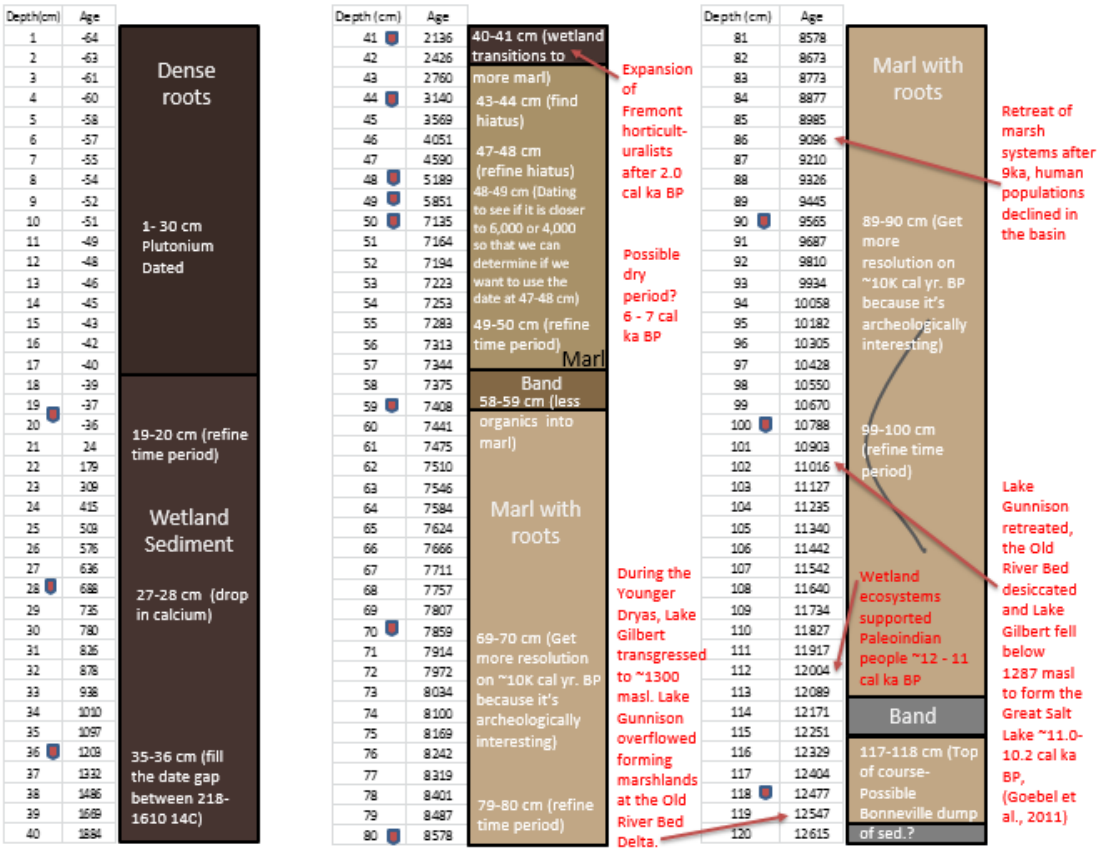

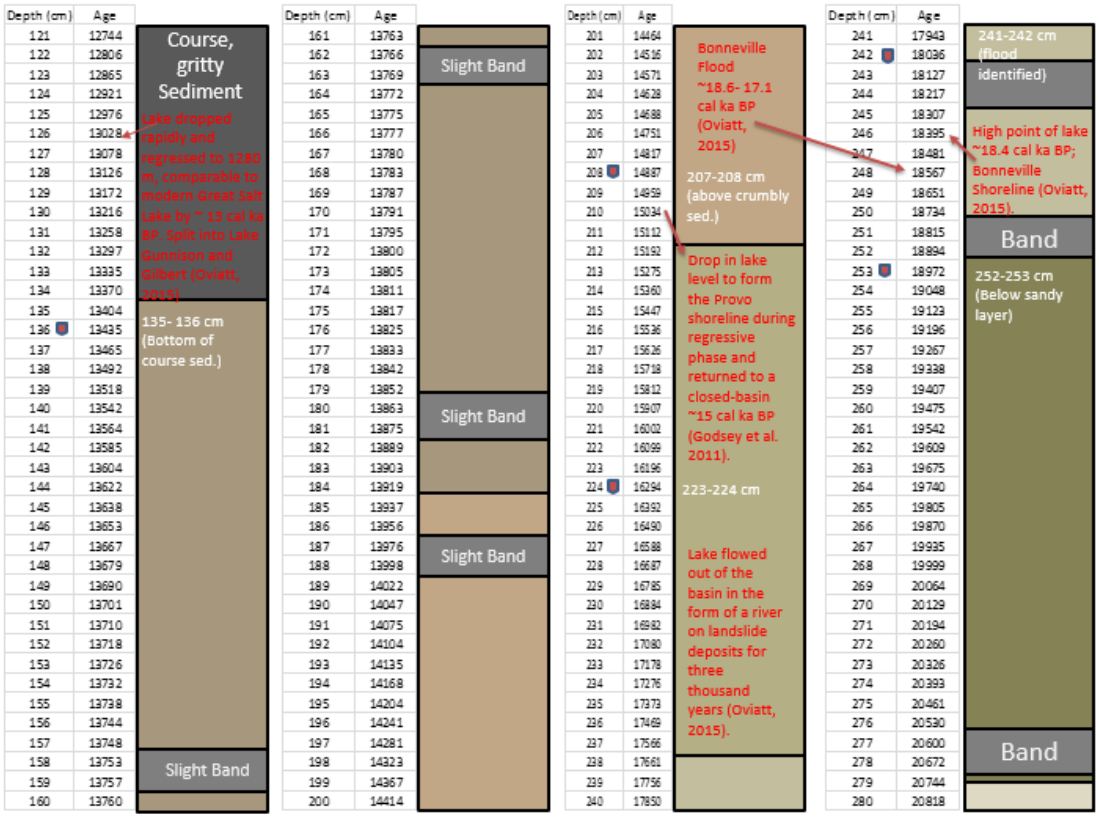
Depth (cm)
Age
Course, gritty Sediment
Lake dropped rapidly and regressed to 1280 m, comparable to modern Great Salt Lake by ~13 cal ka BP. Split into Lake Gunnison and Gilbert (Oviatt, 2015)
135- 136 cm (Bottom of course sed.)
Slight Band
Slight Band
Slight Band
Slight Band
Bonneville Flood ~18.6- 17.1 cal ka BP (Oviatt, 2015)
207-208 cm (above crumbly sed.)
Drop in lake level to form the Provo shoreline during regressive phase and returned to a closed-basin ~15 cal ka BP (Godsey et al. 2011).
223-224 cm
Lake flowed out of the basin in the form of a river on landslide deposits for three thousand years (Oviatt, 2015).
241-242 cm (flood identified)
High point of lake ~18.4 cal ka BP; Bonneville Shoreline (Oviatt, 2015).
Band
252-253 cm (Below sandy layer)
Band

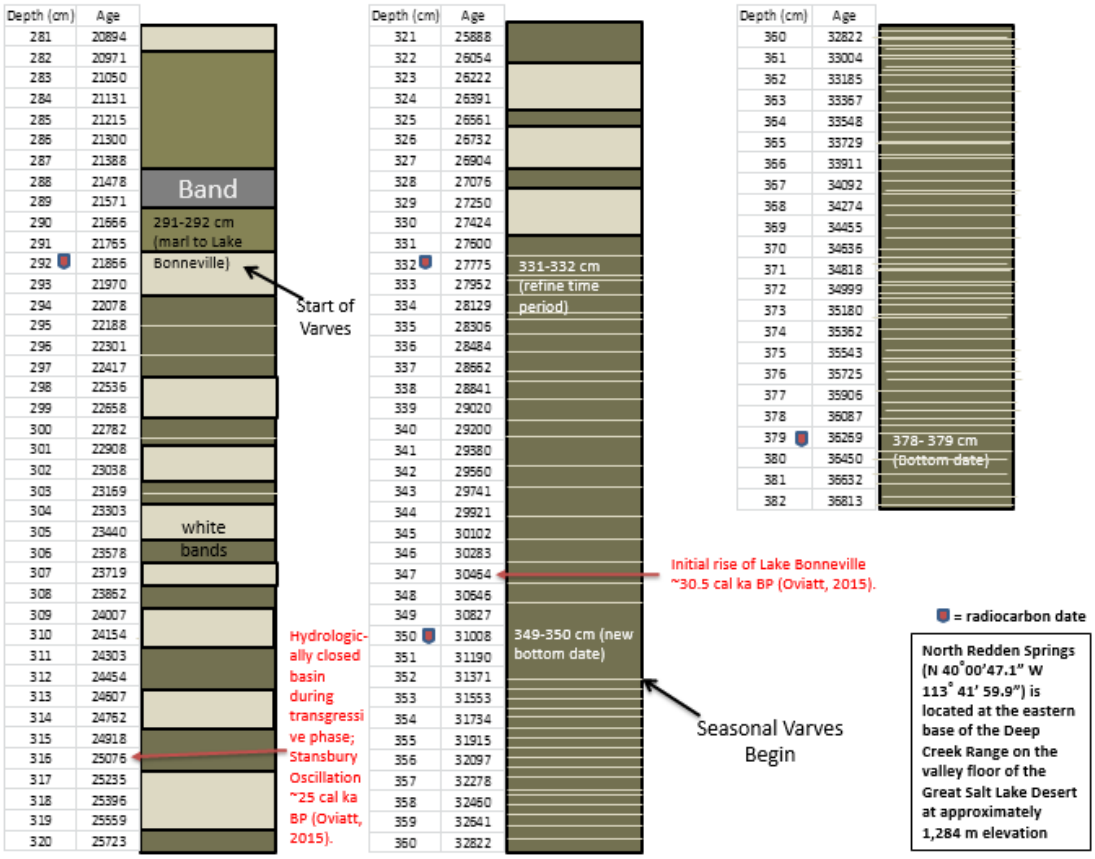
Depth (cm) Age
281 20894
282 20971
283 21050
284 21131
285 21215
286 21300
287 21388
288 21478
289 21571
290 21666
291 21765
292 21866
293 21970
294 22078
295 22188
296 22301
297 22417
298 22536
299 22658
300 22782
301 22908
302 23038
303 23169
304 23303
305 23440
306 23578
307 23719
308 23862
309 24007
310 24154
311 24303
312 24454
313 24607
314 24762
315 24918
316 25076
317 25235
318 25396
319 25559
320 25723
Band
291-292 cm (marl to Lake Bonneville)
white bands
Start of Varves
Hydrologic-ally closed basin during transgressi ve phase; Stansbury Oscillation ~25 cal ka BP (Oviatt, 2015).
Depth (cm) Age
321 25888
322 26054
323 26222
324 26391
325 26561
326 26732
327 26904
328 27076
329 27250
330 27424
331 27600
332 27775
333 27952
334 28129
335 28306
336 28484
337 28662
338 28841
339 29020
340 29200
341 29380
342 29560
343 29741
344 29921
345 30102
346 30283
347 30464
348 30646
349 30827
350 31008
351 31190
352 31371
353 31553
354 31734
355 31915
356 32097
357 32278
358 32460
359 32641
360 32822
331-332 cm (refine time period)
349-350 cm (new bottom date)
Initial rise of Lake Bonneville ~30.5 cal ka BP (Oviatt, 2015).
Seasonal Varves Begin
Depth (cm) Age
360 32822
361 33004
362 33185
363 33367
364 33548
365 33729
366 33911
367 34092
368 34274
369 34455
370 34636
371 34818
372 34999
373 35180
374 35362
375 35543
376 35725
377 35906
378 36087
379 36269
380 36450
381 36632
382 36813
378- 379 cm (Bottom date)
= radiocarbon date
North Redden Springs (N 40°00'47.1" W 113° 41' 59.9") is located at the eastern base of the Deep Creek Range on the valley floor of the Great Salt Lake Desert at approximately 1,284 m elevation

REFERENCES

Antevs, E. (1948). Climatic changes and pre-white man. The Great Basin, with emphasis on glacial and postglacial times. *Bulletin of the University of Utah*, *38*, p. 167-191.

Antevs, E. (1955). Geologic-climatic dating in the West. *American Antiquity*, *20*, p. 317-335.

Beiswenger, J. M. (1991). Late Quaternary vegetational history of Grays Lake, Idaho. *Ecological Monographs, 61*, 165-182.

Benson, L., Lund, S., Smoot, J., Rhode, D., Spencer, R., Verosub, K., Negrini, R. (2011). The rise and fall of Lake Bonneville between 45 and 10.5 ka. *Quaternary International*, *235*(1/2), 57-69. Doi:10.1016/j.quaint.2010.12.014

Bensen, L. V., Kashgarian, M., Rye, R., Lund, S., Paillet, F., Smoot, J., Kester, C., Mensing, S., Meko, D, Lindstrom, S. (2002). Holocene multidecadal and multicentennial droughts affecting northern California and Nevada. *Quaternary Science Revi*ews, *21*, 659-682.

Blaauw, M. (2010). Methods and code for 'classical' age-modelling of radiocarbon sequences. *Quaternary Geochronology*, *5*(5), 512-518.

Bischoff, J. L., Fitts, J. P., Fitzpatrick, J. A. (1997). Responses of sediment geochemistry to climate change in Owens Lake sediment: an 800-k.y. record of saline/fresh cycles in core OL-92. Geological Society of America Special Paper 317, 37–48.

Bond, G. C., & Lotti, R. (1995). Iceberg discharges into the North Atlantic on millennial time scales during the last glaciation. *Science*, *267*(5200), 1005-1010.

Bright, R. C. (1966). Pollen and seed stratigraphy of Swan Lake, southeastern Idaho: it's relation to regional vegetational history and to Lake Bonneville history. *Tebiwa*, *9*, 1-47.

Broughton, J. M. (2000). Terminal Pleistocene fish remains from Homestead Cave, Utah, and implications for fish biogeography in the Bonneville Basin. *Copeia, 3*, 645-656.

Broughton, J. M., Madsen, D. B., & Quade, J. (2000). Fish remains from Homestead Cave and lake levels of the past 13,000 years in the Bonneville Basin. *Quaternary Research*, *53*(3), 392-401.

Clark, J. S. (1988). Particle motion and the theory of stratigraphic charcoal analysis: Source area, transportation, deposition, and sampling. *Quaternary Research*, *30*, 81-91.

Clausing, A. (1999). Palaeoenvironmental significance of the green alga Botryococcus in the lacustrine rotliegend (upper carboniferous-lower permian). *Historical Biology*, *13*(2-3), 221-234.

Currey, D. R. (1990). Quaternary palaeolakes in the evolution of semidesert basins, with special emphasis on Lake Bonneville and the Great Basin, USA. *Palaeogeography, Palaeoclimatology, Palaeoecology*, *76*(3), 189-214.

Currey, D. R. (1991). Hemiarid lake basins—hydrographic and geomorphic patterns: University of Utah Limnotectonic Laboratory Technical Report no. 91-2, 76 p.

Currey, D. R., Steven, R. J. (1982). Paleo environments of the Northeastern Great Basin and Northeastern Basin Rim Region: A Review of Geological and Biological Evidence, in Man and Environment in the Great Basin, ed. by David B. Madsen and James F. O'Connell SAA Papers No.2 pp. 27-52.

Currey, D. R., Oviatt, C.G (1985). Durations, average rates, and probable causes of Lake Bonneville expansions, stillstands, and contractions during the last deep-lake cycle 32,000 to 10,000 years ago. *Geographical Journal of Korea,* V. 10, P. 1085-1099.

Currey, D. R., Oviatt, C.G., Plyer, G.B. (1983). Lake Bonneville stratigraphy, geomorphology, and isostatic deformation in west-central Utah. In Gurgel, K.D. (ed): *Geologic Excursions in Neotectonics and Engineering Geology in Utah, Guidebook-Part IV, 63-82. Utah Geological and Mineral Survey Special Studies 62*, Utah Geological and Mineral Survey, Salt Lake City, UT.

Davis, O.K. (2002). Neogene environmental history of the northern Bonneville basin: A review of palynological studies. In: Hershler, R., Madsen, D.B., Currey, D.R. (Eds.), Great Basin Aquatic Systems History. Smithsonian Contributions to the Earth Sciences, vol. 33. Smithsonian Institute Press, Washington, D.C., pp. 295-307.

Dean J, W. E. (1974). Determination of carbonate and organic matter in calcareous sediments and sedimentary rocks by loss on ignition: comparison with other methods. *Journal of Sedimentary Research*, *44*(1), 242-248.

Eardley, A.J., Shuey, R.T., Gvosdetsky, V., Nash, W. P., Picard, M. D., Grey, D. C., Kukla, G.J. (1973). Lake cycles in the Bonneville Basin, Utah. *Geological Society of America Bulletin, 84*, 211-216.

Eckerle, W., Brunelle, A., Rhode, D., Macharia, A.N., Mayer, J., Petersen, K., Power, M.J., Rogers, O., Spencer, J., Taddie, S., Louderback, L.A. (2013). Ruby Natural Gas Pipeline-Northern Utah. Federal Energy Regulatory Commission and the Bureau of Land Management. Volume 3: Paleoenvironmental Studies.

Faegri, K., Iversen, J., Kaland, P.E., Krzywinski, K. (1989). *Textbook of pollen analysis*. 4th edition. Wiley, New York.

Fowler, D. D. (Ed.). (1977). *Models and Great Basin Prehistory: A Symposium*. Desert Research Institute.

Gardner, J. J., & WhitloFck, C. (2001). Charcoal accumulation following a recent fire in the Cascade Range, northwestern USA, and its relevance for fire-history studies. *The Holocene, 11*(5), 541-549.

Gilbert, G.K. (1890). Lake Bonneville: U.S. Geological Survey Monograph 1, p. 438.

Godsey, H. S., Currey, D. R., Chan, M. A. (2005). New evidence for an extended occupation of the Provo shoreline and implications for regional climate change, Pleistocene Lake Bonneville, Utah, USA. *Quaternary Research*, 63(2), 212-223. doi: 10.1016/j.yqres.2005.01.002.

Godsey, H. S., Oviatt, C. G., Miller, D. M., & Chan, M. A. (2011). Stratigraphy and chronology of offshore to nearshore deposits associated with the Provo shoreline, Pleistocene Lake Bonneville, Utah. *Palaeogeography, Palaeoclimatology, Palaeoecology*, *310*(3), 442-450.

Goebel, T., Hockett, B., Adams, K. D., Rhode, D., Graf, K. (2011). Climate, environment, and humans in North America's Great Basin during the Younger Dryas, 12,900–11,600 calendar years ago. *Quaternary International*, *242*(2), 479-501. doi:10.1016/j.quaint.2011.03.043.

Google Inc. (2015). Google Earth (Version 5.1.3533.1731) [Software]. Available from https://www.google.com/earth/

Grayson, D. K. (1998). Moisture history and small mammal community richness during the latest Pleistocene and Holocene, northern Bonneville Basin, Utah. *Quaternary Research*, *49*(3), 330-334.

Grayson, D. K. (2000a). The Homestead cave mammals. In: Madsen, D.B. (Ed.), *Late Quaternary Paleoecology in the Bonneville Basin, Bulletin*, *130*, 67-89. Salt Lake City.

Grayson, D. K. (2000b). Mammalian responses to Middle Holocene climatic change in the Great Basin of the western United States. *Journal of Biogeography*, *27*(1), 181-192.

Grimm, E. (1987). CONISS: A fortran 77 program for stratigraphically constrained cluster analysis by the method of Incremental sum of squares. *Computer and Geosciences*, 13(1) (1987), pp. 13-35.

Hemming, S. R. (2004). Heinrich events: Massive late Pleistocene detritus layers of the North Atlantic and their global climate imprint. *Reviews of Geophysics*, *42*(1).

Higuera, P.E., Brubaker, L.B., Anderson, P.M., Hu, F.S., Brown, T.A. (2009). Vegetation mediated the impacts of postglacial climate change on fire regimes in the south-central Brooks Range, Alaska. *Ecological Monographs 7*(2), 201-219.

Hostetler, S., & Giorgi, F. (1994). Lake-atmosphere feedbacks associated with paleolakes Bonneville and Lahontan. *Science*, *263*(5147), 665.

Huerta, M.A., Whitlock, C., Yale, J. (2009). Holocene vegetation-fire-climate linkages in northern Yellowstone National Park, USA. *Palaeogeography, Palaeoclimatology, Palaeoecology 271*, 170-181.

Jiménez-Moreno, G., Scott Anderson, R., Fawcett, P. J. (2007). Orbital- and millennial-scale vegetation and climate changes of the past 225ka from Bear Lake, Utah–Idaho (USA). *Quaternary Science Reviews*, *26*(13/14), 1713-1724. doi:10.1016/j.quascirev.2007.05.001

Kaufman, D. (2003). Amino acid paleothermometry of Quaternary ostracodes from the Bonneville Basin, Utah. *Quaternary Science Reviews*, *22*, 899-914

Laabs, B.J.C., Refsnider, K.A., Munroe, J.S., Mickelson, D.M., Applegate, P.J., Singer, B.S. Caffee, M. W. (2009). Latest Pleistocene glacial chronology of the Uintah Mountains: Support for moisture-driven asynchrony of the last deglaciation. *Quaternary Science Reviews 28*, 1171-1187.

Louderback, L. A., Rhode, D. E. (2009). 15,000 years of vegetation change in the Bonneville basin: The Blue Lake pollen record. *Quaternary Science Reviews* 28, 308-326.

Louderback, L. A., Grayson, D. K., Llobera, M. (2010). Middle-Holocene climates and human population densities in the Great Basin, western USA. *The Holocene*.

Lyle, M., Heusser, L., Ravelo, C., Yamamoto, M., Barron, J., Diffenbaugh, N. S., ... & Andreasen, D. (2012). Out of the tropics: The Pacific, Great Basin Lakes, and Late Pleistocene water cycle in the western United States. *Science*, *337*(6102), 1629-1633.

Madsen, D.B. (2000). Late Quaternary paleoecology in the Bonneville basin. In: Utah Geological Survey Bulletin, vol.130 Salt Lake City.

Madsen, D. B., Currey, D.R. (1979). Late Quaternary glacial and vegetation changes, Little Cottonwood Canyon area, Wasatch Mountains, Utah. *Quaternary Research 12,* 254-270.

Madsen, D. B., Rhode, D., Grayson, D. K., Broughton, J. M., Livingston, S. D., Hunt, J., & Shaver, M. W. (2001). Late Quaternary environmental change in the Bonneville basin, western USA. *Palaeogeography, Palaeoclimatology, Palaeoecology*, *167*(3), 243-271.

Malde, H.E. (1968). The catastrophic late Pleistocene Bonneville Flood in the Snake River Plain, Idaho. *US Geological Survey Professional Paper* 596, 52 pp.

Massimino, J., Metcalfe, D. (1999). New form for the formative. *Utah Archaeology*, *12*, 1-16.

McGee, D., Quade, J., Edwards, R., Broecker, W., Cheng, H., Reiners, P., Evenson, N. (2012). Lacustrine cave carbonates: Novel archives of paleohydrologic change in the Bonneville basin (Utah, USA). *Earth and Planetary Science Letters 351-352*, 182-194.

Mehringer, P.J. (1985). Quaternary pollen records from the interior pacific northwest and northern Great Basin of the United States. In: Bryant, V.M., Holloway, R. M. (Eds.), Pollen Records of Late-Quaternary North American Sediments. *American Association of Stratigraphic Palynologists*, pp. 168-189.

Mensing, S. A., Benson, L. V., Kashgarian, M., Lund, S. (2004). A Holocene pollen record of persistent droughts from Pyramid Lake, Nevada, USA. *Quaternary Research, 62*(1), 29-38.

Mensing, S., Livingston, S., and Barker, P. (2006). Long-term fire history in Great Basin sagebrush reconstructed from macroscopic charcoal in spring sediments, Newark Valley, Nevada. *Western North American Naturalist, 66,* 64-77.

Mensing, S., Smith, J., Burkle Norman, K., Allan, M. (2008). Extended drought in the Great Basin of western North America in the last two millennia reconstructed from pollen records. *Quaternary International, 188*, 79-89.

Minckley, T. A., Bartlein, P. J., Whitlock, C., Shuman, B. N., Williams, J. W., Davis, O. K. (2008). Associations among modern pollen, vegetation, and climate in western North America. *Quaternary Science Reviews, 27*(21), 1962-1991.

Munroe, J. S., Laabst, B. C., Shakun, J. D., Singer, B. S., Mickelson, D. M., Refsnider, K. A., Caffee, M. W. (2006). Latest Pleistocene advance of alpine glaciers in the southwestern Uinta Mountains, Utah, USA: Evidence for the influence of local

moisture sources. *Geology*, *34*(10), 841-844. doi:10.1130/G22681.1

Nagler, P.L., Glenn, E.P., Jarnevich, C.S., Shafroth, P.B. (2011). Distribution and abundance of saltcedar and Russian olive in the western United States. *Critical Reviews in Plant Science, 30*(6): 508-523.

Nishizawa, S., Currey, D. R., Brunelle, A., Sack, D. (2013). Bonneville basin shoreline records of large lake intervals during Marine Isotope Stage 3 and the Last Glacial Maximum. *Palaeogeography, Palaeoclimatology, Palaeoecology*, *386*, 374-391. doi:10.1016/j.palaeo.2013.05.034

NOAA National Climatic Data Center. (2015). Index of Paleo Climate Forcing [Data File]. Retrieved from http://www1.ncdc.noaa.gov/pub/data/paleo/climate_forcing/orbital_variations/berger_insolation/

Oviatt, C. G. (2015). Chronology of Lake Bonneville, 30,000 to 10,000 yr B.P. *Quaternary Science Reviews*, *110*, 166-171. doi:10.1016/j.quascirev.2014.12.016

Oviatt, C.G. (1997). Lake Bonneville fluctuations and global climate change. *Geology, 25*, 155-158.

Oviatt, C.G., Currey, D.R. Sack, D. (1992). Radiocarbon chronology of Lake Bonneville, eastern Great Basin, USA. *Palaeogeography, Palaeoclimatology, Pala*eoecology, *99*, 225-241.

Oviatt, C. G., Madsen, D. B., Schmitt, D. N. (2003). Late Pleistocene and early Holocene rivers and wetlands in the Bonneville basin of western North America. *Quaternary Research*, *60*(2), 200. doi:10.1016/S0033-5894(03)00084-X

Oviatt, C. G., Miller, D. M., McGeehin, J. P., Zachary, C., & Mahan, S. (2005). The Younger Dryas phase of Great Salt Lake, Utah, USA. *Palaeogeography, Palaeoclimatology, Palaeoecology*, *219*(3/4), 263-284. doi:10.1016/j.palaeo.2004.12.029

Patrickson, S. J., Sack, D., Brunelle, A. R., Moser, K. A. (2010). Late Pleistocene to early Holocene lake level and paleoclimate insights from Stansbury Island, Bonneville basin, Utah. *Quaternary Research, 73*(2), 237-246. doi:10.1016/j.yqres.2009.12.006

Reheis, M. C., Adams, K. D., Oviatt, C. G., Bacon, S. N. (2014). Pluvial lakes in the Great Basin of the western United States-a view from the outcrop. *Quaternary Science Reviews*, *97*, 33-57. doi:10.1016/j.quascirev.2014.04.012

Rhode, D. (2000a). Middle and late Wisconsin vegetation in the Bonneville basin. In: Madsen, D.B. Ed.), Late Quaternary Paleoecology in the Bonneville Basin. Utah

Geological Survey Bulletin, vol. 130, pp.137-247. Salt Lake City.

Rhode, D. (2000b). Holocene vegetation history in the Bonneville basin. In: Madsen, D.B. (Ed.), Late Quaternary Paleoecology in the Bonneville Basin. Utah Geological Survey Bulletin, vol. 130, pp. 149-163, Salt Lake City.

Rhode, D., Madsen, D.B. (1995a). Late Wisconsin vegetation in the northern Bonneville basin. *Quaternary Research*, *44*, 246-256.

Rhode, D., Madsen, D.B. (1995b). Early Holocene vegetation in the Bonneville basin. *Quaternary Research*, *44*, 246-256.

Rhode, D., Goebel, T.E., Graf, K.E., Hockett, B.S., Jones, K.T., Madsen, D.B., Oviatt, C.G., Schmitt, D.N. (2005). Latest Pleistocene- early Holocene human occupation and paleoenvironmental change in the Bonneville basin, Utah-Nevada. In: Pederson, J., Dehler, C.M. (Eds.), Interior Western United States. Geological Society of America Field Guide, vol 6, pp. 211-230, Boulder, CO.

Schmitt, D. N., Madsen, D. B., Lupo, K. D. (2002). Small-mammal data on early and middle Holocene climates and biotic communities in the Bonneville Basin, USA. *Quaternary Research*, *58*(3), 255-260.

Scott, W. E., McCoy, W. D., Shroba, R. R., Rubin, M. (1983). Reinterpretation of the exposed record of the last two cycles of Lake Bonneville, western U.S. *Quaternary Research*, *20*, 261-285.

Spencer, R.J., Baedecker, M., Eugster, H.P., Forester, R.M., Goldhaber, M.B., Jones, B.F., Kelts, K., MacKenzie, J., Madsen, D.B., Rettig, S.L., Rubin, M., Browser, C.J. (1984). Great Salt Lake and precursors, Utah: the last 30,000 years. *Contributions to Mineralogy and Petrology*, *86*, 321-334.

Tausch, R. J., Nowak, C. L., & Mensing, S. A. (2004). Climate change and associated vegetation dynamics during the Holocene: the paleoecological record. *Great Basin riparian ecosystems: Ecology, management and restoration*, 24-48.

Thompson, R.S. (1990). Late Quaternary vegetation and climate in the Great Basin. *Packrat middens: The last 40,000 years of biotic change*, 201-239.

Thompson, R.S. (1992). Late Quaternary environments in Ruby Valley, Nevada. *Quaternary Research*, *37*, 1-15.

Wetzel, R. G. (2001). *Limnology: Lake and river ecosystems*. Academic Press, San Diego.

Whitlock, C., Millspaugh, S.H. (1996). Testing the assumptions of fire-history studies: an examination of modern charcoal accumulation in Yellowstone National Park,

USA. *The Holocene*, *6*, 7-15.

Wigand, P. E. (1987). Diamond Pond, Harney County, Oregon: vegetation history and water table in the eastern Oregon desert. *The Great Basin Naturalist, 47*, 427-458.

Wigand, P., Rhode, D. (2002). Great Basin vegetation history and aquatic systems: the last 150,000 years. In: Hershler, R., Madsen, D.B., Currey, D.R. (Eds.), Great Basin Aquatic Systems History. Smithsonian Contributions to the Earth Sciences, vol. 33. Smithsonian Institute Press, Washington, D.C., pp. 309-368.

Williams, J., Shuman, B., Bartlein, P., Whitmore, J., Gajewski, K., Sawada, M., Minckley, T., Shafer, S., Viau, A., Webb III, T., Anderson, P., Brubaker, L., Whitlock, C., & Davis, O. (2006). Atlas of Pollen-Vegetation-Climate Relationships for the United States and Canada**.** *American Association of Stratigraphic Palynologists.* Contribution Series No. 43. Retrieved from http://www.ncdc.noaa.gov/paleo/pubs/williams2006/williams2006.html

Zic, M., Negrini, R. M., Wigand, P. E. (2002). Evidence of synchronous climate change across the Northern Hemisphere between the North Atlantic and the northwestern Great Basin, United States. *Geology*, *30*(7), 635-638.

Zolitschka, B., Mingram, J., Van Der Gaast, S., Jansen, J. F., & Naumann, R. (2001). Sediment logging techniques. In *Tracking environmental change using lake sediments* (pp. 137-153). Springer, Netherlands.